showing a normal cycle received an OVX under isoflurane anesthesia. One week after OVX, all animals were subcutaneously treated with 2 μg/rat of estradiol benzoate (EB) at 9:00 for 3 consecutive days and 500 μg/rat of progesterone (P4) at 11:00 of the last day of EB treatment for artificial LH surge priming. For the time-course analysis, all animals were decapitated at 11:00 (soon after P4 injection), 14:00, 15:00, 16:00, 17:00 and 19:00 (n = 5–7/time point) of the LH surge priming day and blood samples were collected. The middle-age group was maintained until 22 weeks of age with daily observation of estrous cycle, then divided into 2 groups, one with normal estrous cycle (Middle (N) group, n = 5/time point, total 30 females/group) and another with persistent estrus (Middle (PE) group, n = 4/time point, total 16 females/group). Both groups received the same OVX and LH surge priming treatment and were decapitated at the same times as the control and EE groups, without the time points of 11:00 and 19:00 in the Middle (PE) group. These middle-aged groups were prepared as the animals with spontaneous reproductive aging, and this strain is known to show persistent estrus starting from approximately 4 months of age [8]. Brains were removed from the skulls, and the hypothalami were dissected out as described in a previous report [34] using a horizontal cut about 2 mm in depth with the following 3 limits: 1 mm anterior to the optic chiasm as anterior limit, the posterior end of mammary bodies as posterior limit, and the hypothalamic fissures as lateral limit. Dissected hypothalami were macroscopically divided using the optic chiasm as a boundary into anterior and posterior hypothalamus, which included the AVPV and the ARC, respectively. The hypothalamic samples were immediately frozen in liquid nitrogen and stored at −80 °C until the time of RNA isolation. The uterus, vagina and mammary glands were also resected from each animal. All organs were fixed in 10% neutral buffered formalin. Tissues were processed routinely and stained with hematoxylin and eosin (HE) for histopathologic examination.

2.4. Hormone assays

Serum samples obtained from decapitation were stored at −80 °C before assay. The serum concentrations of follicle-stimulating hormone (FSH) and LH were determined using double-antibody radioimmunoassays and 125I-labeled radio-ligands. National Digestive and Kidney Disease (NIDDK) radioimmunoassay kits were used for rat FSH and LH with anti-rat LH-S-11 and anti-rat FSH-S-11, as described previously [35]. The intra- and inter-assay coefficients of variations were: 5.09% and 20.75%; 3.45% and 17.40% for FSH and LH, respectively.

2.5. Quantitative real-time PCR

Total RNA was extracted from the hypothalamus lysates using ISOGEN (Nippon Gene Co. Ltd., Tokyo, Japan), and reverse transcription reactions were performed using 1 μg of total RNA with High Capacity Reverse Transcription kits (Applied Biosystems, Foster City, CA, USA). Following the manufacturer's instructions, real-time PCR (7900HT Fast Real-time PCR System, Applied

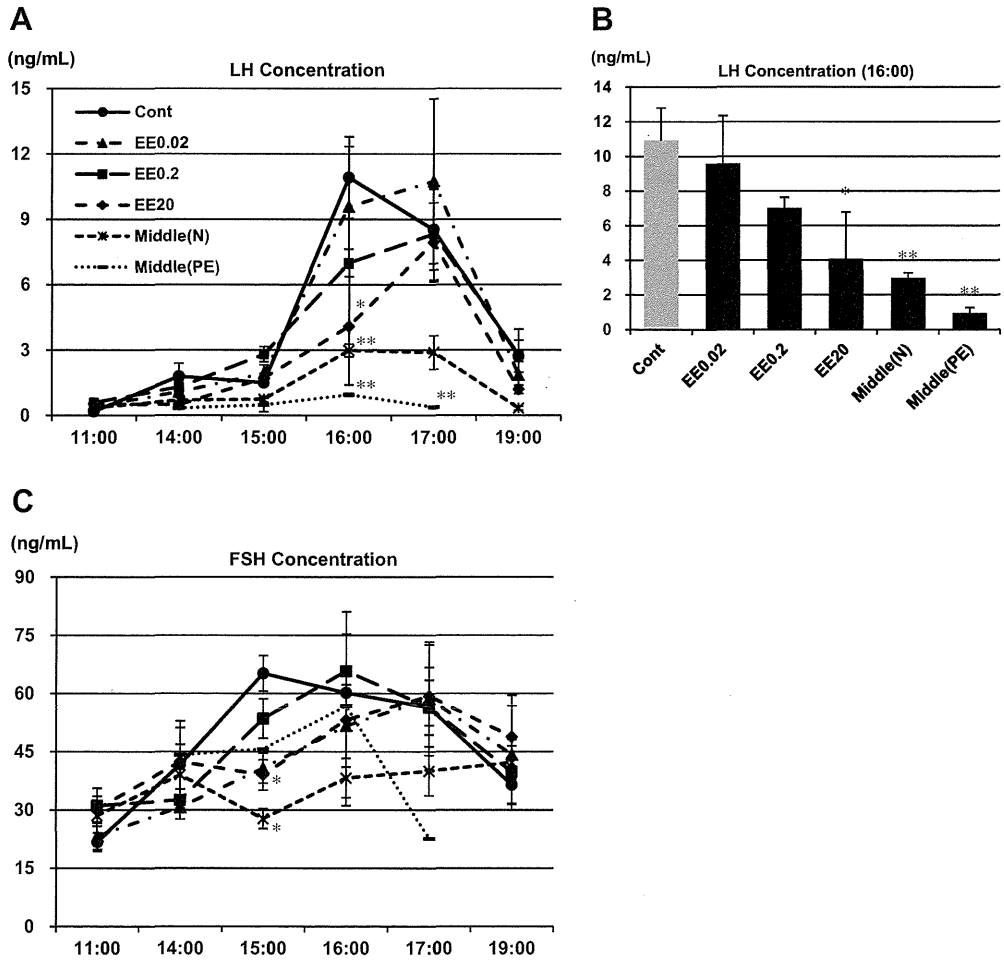

Fig. 1. Sequential changes in serum LH (A) and FSH (C) concentration in EE-exposed and middle-age groups and intergroup comparison of LH concentration at 16:00 (B). EE-exposed groups showed dose-dependent decrease in peak area and concentration of LH at 16:00, and this decrease was more evident in both middle-age groups. Data are presented as mean ± S.E. or mean + S.E. (n = 4–7/group). Symbols indicate significant difference from control group (*p < 0.05 and **p < 0.01 by Dunnett's test, respectively).

Biosystems) was performed using TaqMan® Fast Universal PCR Master Mix (Applied Biosystems) and TaqMan® Gene Expression Assays (Applied Biosystems) as primer–probe sets for the following genes: *KiSS1* (KiSS1, Rn00710914_m1), *KiSS1r* (KiSS1R, Rn00576940_m1), *Esr1* (ERα, Rn01640372_m1), *Esr2* (ERβ, Rn00562610_m1) and *Fos* (c-fos, Rn00487426_g1). The expression level of each gene was calculated by the relative standard curve method and normalized against endogenous GAPDH (TaqMan Rodent GAPDH Control Reagent, Applied Biosystems).

2.6. Experiment 2

For further assessment of kisspeptin neurons, we conducted another experiment to obtain brain samples for in situ hybridization. Dams were assigned to 5 groups (4–9 dams/group). All pups were processed as in *Experiment 1* with subcutaneous injection of EE on PND0 for artificial LH surge priming at 11 weeks of age. On the LH surge priming date, all animals were deeply anesthetized with pentobarbital sodium (Kyoritsu Seiyaku Corporation, Tokyo, Japan) and transcardially perfused with saline followed by 4% paraformaldehyde (PFA, Nacalai Tesque, Inc., Kyoto, Japan) during the interval from 16:00 to 17:00 ($n = 4$/group). Brains were removed immediately and post-fixed in 4% PFA overnight at 4 °C, then immersed in 30% sucrose/PBS solution at 4 °C until tissues sank. The fixed brains were embedded in O.C.T. compound (Sakura Finetek Japan Co. Ltd., Tokyo, Japan) and blocks were stored at −80 °C until sectioning. The uterus, vagina and pituitary were also resected from each animal. All organs were post-fixed in 4% PFA. Tissues were routinely processed and stained with HE for histopathologic examination.

2.7. In situ hybridization (ISH)

Non-radioactive ISH was used for KiSS1 mRNA-positive cell detection with reference to a previous report [36]. Slides were washed with PBS and treated with 1 μg/mL proteinase K (Takara Bio Inc., Shiga, Japan), followed by brief 1% PFA immersion. After

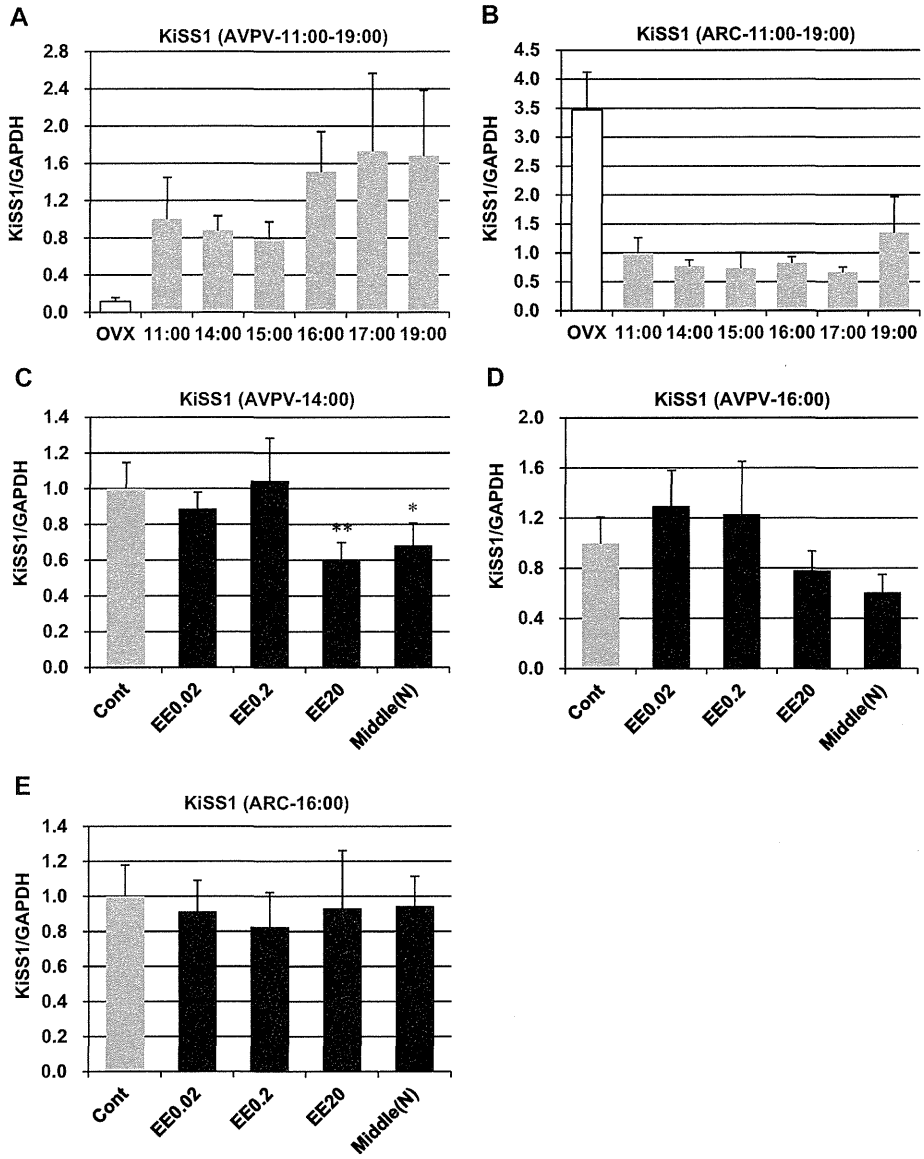

Fig. 2. Sequential changes in KiSS1 mRNA expression in the control group in the AVPV (A) and ARC (B), and intergroup comparison in the AVPV at 14:00 (C) and 16:00 (D) and in the ARC at 16:00 (E). The expression significantly decreased in the EE20 and Middle (N) groups in the AVPV at 14:00, but intergroup differences were not detected in the ARC. All data are presented as mean + S.D. ($n = 5$/group). Expression level at 11:00 (A and B) or control group (C–E) is adjusted to 1.0. The OVX only group was investigated as a negative control. Symbols indicate significant difference from the control group (*$p < 0.05$ and **$p < 0.01$ by Dunnett's test, respectively).

washing in PBS, slides were incubated with 0.25% acetic anhydride in 0.1 M triethanolamine, and then prehybridized with hybridization buffer for 30 min at 60 °C. After prehybridization, slides were hybridized with 0.5 μg/mL of DIG-labeled anti-sense RNA probe (sequence position 3-358, GenBank accession No. AY196983.1, Genostaff, Tokyo, Japan) overnight at 60 °C. A sense RNA probe was used as a negative control. Following hybridization, the slides were washed with 4× SSC/50% formamide, 2× SSC, and 1× SSC. Between SSC washes, slides were briefly immersed in a 20 μg/mL RNase working solution at 37 °C. After washing, slides were blocked with 2% BSA (Sigma, St. Louis, MO, USA) in ISH buffer-1 and incubated with anti-DIG antibody (1:1000, Roche Applied Science, Mannheim, Germany) in ISH buffer-1. Following washing with ISH buffer-1, the slides were immersed in ISH buffer-3 [100 mM Tris–HCl (pH 9.5), 100 mM NaCl, and 50 mM $MgCl_2$] and then incubated with NBT/BCIP solution (Roche Applied Science) in ISH buffer-3 for 1 h.

2.8. Dual-labeling ISH/immunohistochemistry (IHC)

Following ISH for KiSS1 mRNA, the sections were treated with 1% BSA (Sigma, St. Louis, MO, USA) in PBS and incubated with rabbit anti-ERα (1:2000, sc-542, Santa Cruz Biotechnology Inc., CA, USA) or rabbit anti-c-fos (1:4000, sc-253, Santa Cruz Biotechnology Inc.) overnight. A negative control was incubated without primary antibody. After washing with PBS, the sections were incubated with biotin-conjugated goat anti-rabbit IgG (1:200, Vector Laboratories Inc., CA, USA) in 1% BSA for 30 min. Then the sections were incubated with avidin-biotinylated HRP complex (Vectastain Elite ABC kit, Vector Laboratories Inc.) in PBS for 30 min. The sections were visualized with 3,3-diaminobenzidine-tetrachloride (DAB) mixed with hydrogen peroxide in PBS.

2.9. Sectioning and quantitative analysis of positive cells in ISH and dual-labeling ISH/IHC

In order to evaluate the whole area of the AVPV and ARC, we made sequential coronal sections (20 μm thick) of the AVPV from approximately 0.12 mm anterior to 0.24 mm posterior to the bregma, and of the ARC from approximately 1.72 mm posterior to 3.60 mm posterior to the bregma (Paxinos and Watson, The Rat Brain, 6th edition) using a cryostat (Leica, CM1850UV). After sectioning, all tissue sections were immediately mounted on coated slides (Matsunami Glass Ind., Ltd., Osaka, Japan) and then completely air dried and stored at −80 °C before staining. Since 1 section from every 4 sections from the AVPV and every 15 sections from the ARC was chosen for staining, a total of 4 sections for the AVPV and 6 sections for the ARC per rat were examined. For positive cell counting, an Olympus BX51 microscope with an Olympus digital camera DP73 (Olympus, Tokyo, Japan) was utilized. All KiSS1 mRNA-positive cells with visible reactions in ISH and KiSS1-positive cells with or without ERα/c-fos immunoreactivity in dual-labeling ISH/IHC observed in the lateral half of the brain were manually counted at high magnification in a blinded fashion. The total numbers of KiSS1-positive cells and KiSS1-positive cells with ERα/c-fos immunoreactivity in each group were statistically compared. It was confirmed preliminarily that all sections from the AVPV and ARC had approximately the same number of positive cells in each brain half.

2.10. Statistical analysis

Following Bartlett's test, variances in data for the days of vaginal opening, body and organ weights, hormone assays, real-time PCR and numbers and percentages of ISH or dual-labeling ISH/IHC positive cells were compared with those for the control group by

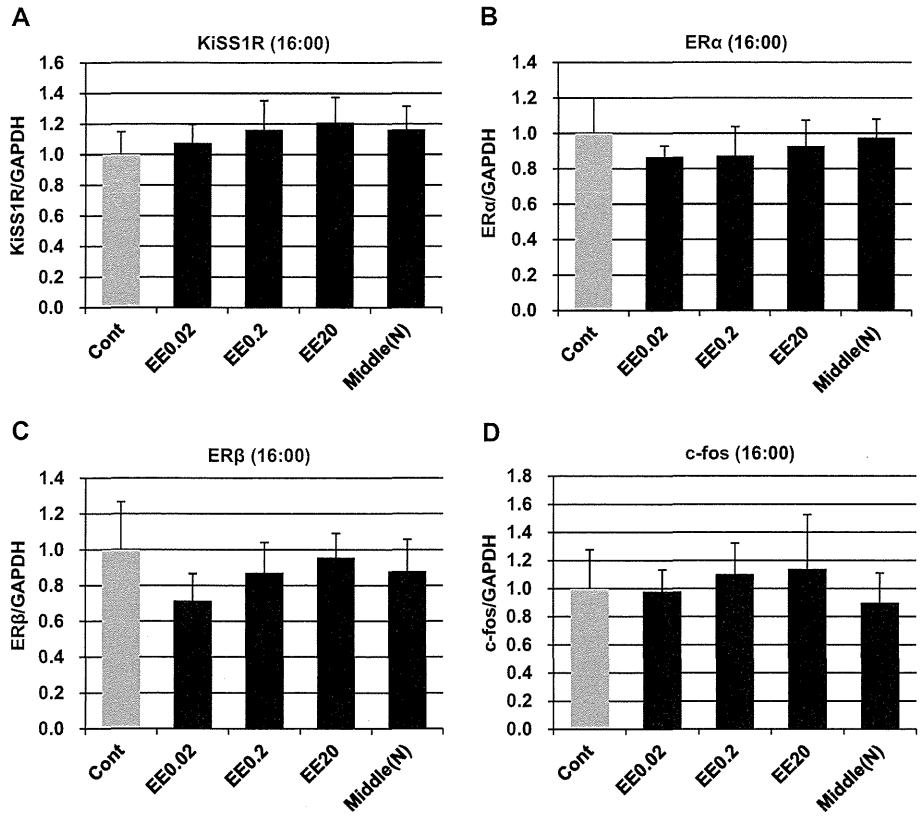

Fig. 3. mRNA expression of KiSS1R (A), ERα (B), ERβ (C), and c-fos (D) in the AVPV at 16:00. No intergroup difference was detected for any KiSS1-related gene. All data are presented as mean+S.D. (n=5/group). Expression level of the control group is adjusted to 1.0.

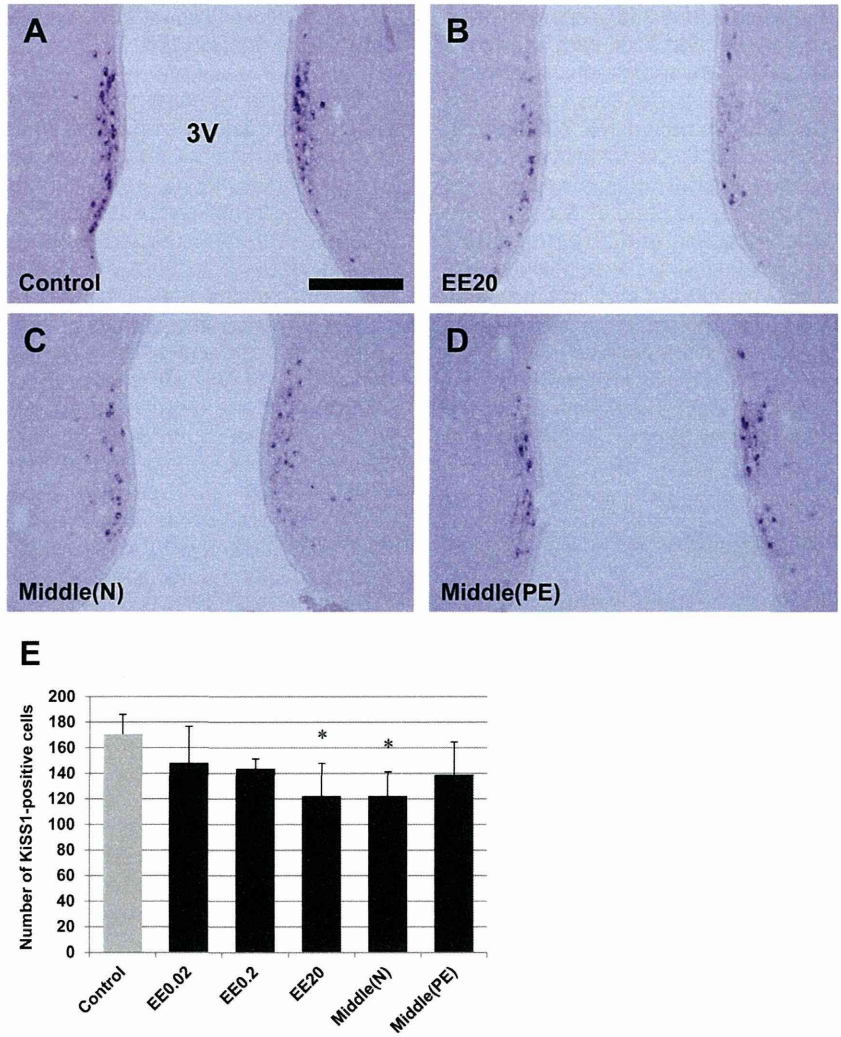

Fig. 4. Representative images of KiSS1 mRNA-positive cells in the AVPV in control (A), EE20 (B), Middle (N) (C) and Middle (PE) (D) groups. The number of positive cells was significantly decreased in the EE20 and Middle (N) groups (E). All brain samples were collected during the interval from 16:00–17:00. All data are presented as mean + S.D. ($n = 4$/group). Symbols indicate significant difference from the control group ($^*p < 0.05$ by Dunnett's test). 3V: third ventricle. Scale bar = 200 μm.

one-way analysis of variance or the Kruskal–Wallis test. When statistically significant differences were detected, Dunnett's multiple comparison test was employed for comparisons among the control group, EE-exposed groups and middle-age groups. In these tests, the level of significance was set at 0.05.

3. Results

3.1. Clinical observation, estrous cycle, and ovarian histology

No abnormalities or deaths were observed throughout the experimental periods. Significant increases in body weight were observed in all EE groups during weeks 4 and 5; however, these changes were transient, and no intergroup differences were observed after week 6 (data not shown). No significant differences were detected in the mean days of vaginal opening between each group (data not shown). All animals, except those in the Middle (PE) group, were confirmed to have normal estrous cycles before OVX by daily observation of vaginal smears. After OVX, vaginal smear showed a pattern similar to that of diestrus in all animals, and cornified smears were observed after EB treatment for 3 days. Estrous cycles determined by ovarian histology coincided well with those determined by vaginal smears, and no histological difference at each cycle was found between the control group and EE-exposed groups. In middle-age groups, several animals in the Middle (N) group showed a decreased number of recent corpora lutea, which may indicate a possibility of occurrence of anovulation status in resent several cycles, although the vaginal smears indicated normal estrous cycles. Most animals in the Middle (PE) group showed a lack of recent corpora lutea and cystic atresia, which reflects prolonging anovulation status in this group.

3.2. Serum concentration of LH and FSH

Sequential changes in serum LH concentrations are shown in Fig. 1. LH concentrations were markedly increased during the interval from 16:00 to 17:00 in the control and EE-exposed groups, but the peak time of LH concentrations were delayed in EE-exposed groups as it detected at 16:00 in the control group and 17:00 in the EE-exposed groups. In the middle-age groups, a slight increase in LH concentrations at 16:00–17:00 was observed in the Middle (N) group, and the Middle (PE) group was almost near the baseline throughout the measurement period. In addition, the peak areas of the LH surges in the EE-exposed and middle-age groups clearly decreased compared to that of the control group. On the other hand, the peak area in the EE0.02 group was almost the same as that detected in the control group (Fig. 1A). In intergroup comparisons at each time point, the serum LH concentrations were significantly

decreased in the EE20, Middle (N) and Middle (PE) groups at 16:00, and a slight decrease was observed in the EE0.2 group (Fig. 1B). Sporadic increases or decreases were also observed at other time points; however, these changes were considered to be incidental due to lack of consistency and dose dependency. Serum FSH concentrations were moderately increased beginning in the afternoon, peaking at 15:00 in the control group and 16:00–17:00 in the EE-exposed groups. A significant decrease was observed in the EE0.02 and EE20 groups at 15:00. The FSH concentration of the Middle (N) group was not increased throughout the measurement period and significantly decreased from the control group at 15:00 (Fig. 1C).

3.3. Quantitative real-time PCR

Sequential changes in KiSS1 mRNA expression in the AVPV and ARC of the control group and intergroup comparisons are shown in Fig. 2. In the AVPV, obvious expression of KiSS1 mRNA was detected from 11:00 and peak expression was observed during the interval from 16:00 to 17:00, the same as the peak time of LH surge in the present study. This peak expression continued to be detected at 19:00 (Fig. 2A). In the ARC, expression of KiSS1 mRNA was suppressed throughout the measured time points when compared to expression in the OVX-only group, and expression slightly recovered at 19:00 (Fig. 2B). Intergroup comparison revealed that KiSS1 mRNA expression in the AVPV of the EE20 and Middle (N) groups was significantly decreased at 14:00, and this decreasing trend continued to be observed in both groups at 16:00, although the decrease was not statistically significant at this time point (Fig. 2C and D). On the other hand, no intergroup differences were detected in KiSS1 mRNA expression in the ARC at 16:00 (Fig. 2E). The mRNA expression of KiSS1-related genes is shown in Fig. 3. Although a clear decrease in KiSS1 mRNA expression in the AVPV was detected in the EE20 and Middle (N) groups, expression of KiSS1R, ERα, and ERβ mRNA was not significantly changed among the control, EE-exposed, or Middle (N) groups (Fig. 3A–C). In addition, c-fos expression, which was examined as a marker of neuronal activity in the kisspeptin neurons, was also not changed among the experimental groups (Fig. 3D).

3.4. In situ hybridization

Representative KiSS1 mRNA-positive cells in the AVPV and ARC are shown in Figs. 4 and 5, respectively. In the AVPV, most KiSS1-positive cells were located around the third ventricle (3V), and the

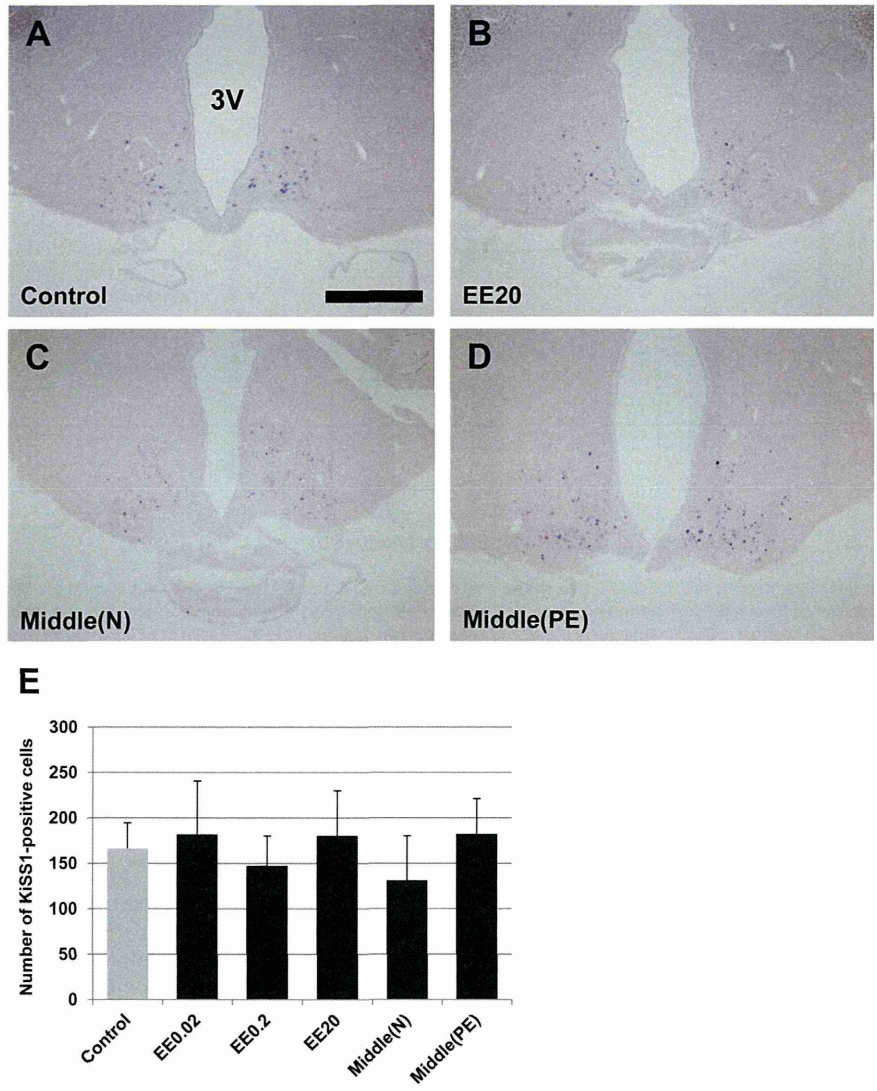

Fig. 5. Representative images of KiSS1 mRNA-positive cells in the ARC in control (A), EE20 (B), Middle (N) (C) and Middle (PE) (D) groups. No intergroup differences in the number of KiSS1-positive cells were detected in the ARC (E). All brain samples were collected during the interval from 16:00 to 17:00. All data are presented as mean + S.D. (n = 4/group). 3V: third ventricle. Scale bar = 500 μm.

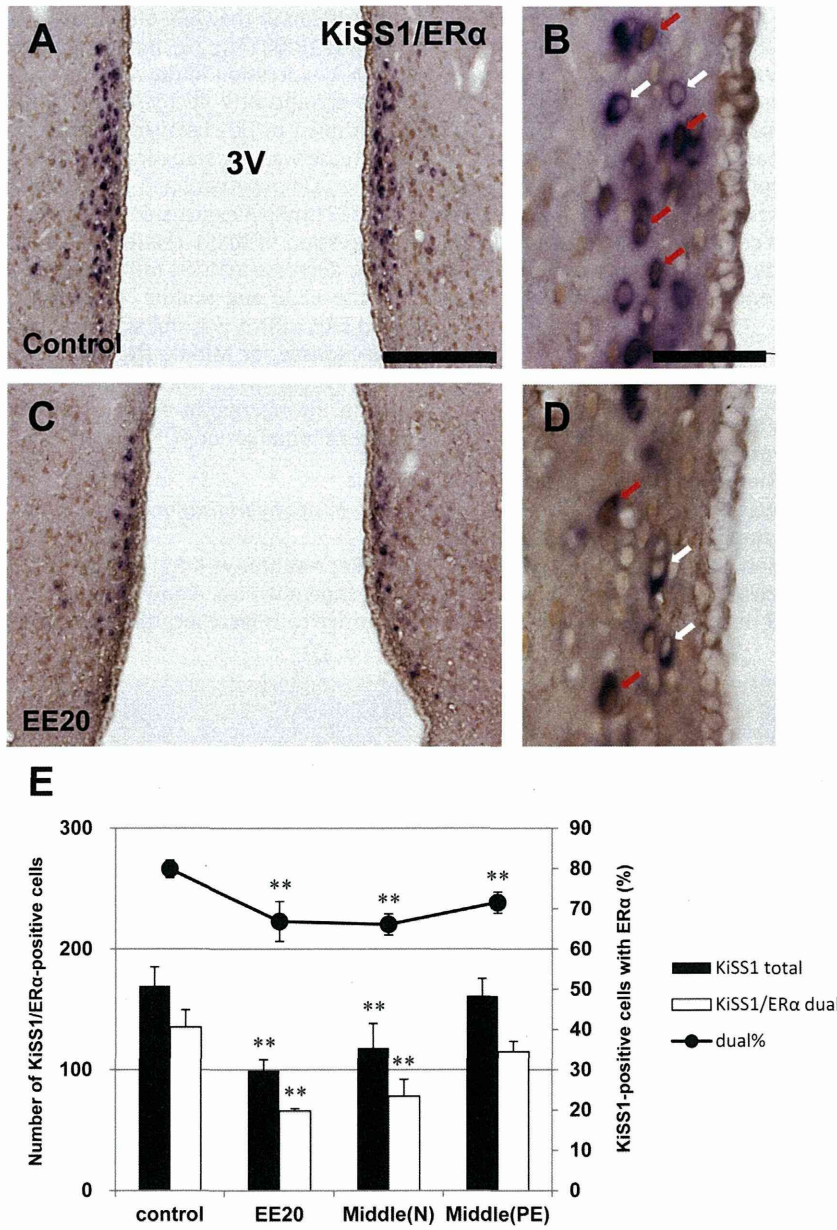

Fig. 6. Representative images of dual-labeling ISH/IHC for KiSS1/ERα in the AVPV in control (A and B) and EE20 (C and D) groups. Most positive cells show dark blue cytoplasimic staining for KiSS1 mRNA and brown nuclear staining for ERα. Red arrows represent KiSS1/ERα-double positive cells and white arrows represent KiSS1 mRNA-single positive cells. Percentage of KiSS1-positive cells showing nuclear ERα immunoreactivity significantly decreased in EE20, Middle (N) and Middle (PE) groups (E). Graph shows the total number of KiSS1-positive cells (closed bar), the number of KiSS1/ERα double positive cells (open bar) and percentage of KiSS1-positive cells showing ERα co-expression (line chart). All brain samples were collected during the interval from 16:00 to 17:00. Data are presented as mean ± S.D. or mean + S.D. ($n = 4$/group). Symbols indicate significant difference from the control group (**: $p < 0.01$ by Dunnett's test). 3 V: third ventricle. Scale bars = 200 μm (A and C) or 50 μm (B and D).

number of KiSS1 mRNA-positive cells (half brain) was significantly decreased in the EE20 and Middle (N) groups and slightly decreased in other EE-exposed groups (Fig. 4E). In addition to decrease in the number of positive cells, attenuation of KiSS1 mRNA signals in each positive cell was observed in the EE20 and Middle (N) groups relative to that in the control group (Fig. 4A–C). Interestingly, on the other hand, KiSS1 mRNA intensity in each positive cell seemed to be slightly recovered in the Middle (PE) group (Fig. 4D). In the ARC, KiSS1 mRNA-positive cells were located in the lower periventricular area of the 3V. In contrast to the AVPV, the number and intensity of KiSS1-positive cells in the ARC were not significantly changed among the control, EE-exposed, or middle-age groups (Fig. 5A–E).

3.5. Dual-labeling ISH/IHC

Representative KiSS1 mRNA-positive cells with ERα/c-fos immunoreactivity are shown in Figs. 6 and 7, respectively. In dual-labeling staining with KiSS1 and ERα/c-fos, dual positive cells showed dark blue cytoplasimic staining for KiSS1 mRNA and brown nuclear staining for ERα/c-fos (red arrows), and KiSS1-single positive cells only showed cytoplasmic staining for KiSS1 (white arrows) (Figs. 6A–D and 7A–D). In dual staining with KiSS1 and ERα, most KiSS1-positive cells showed positive nuclear immunoreactivity for ERα and the percentage of KiSS1-positive cells co-expressing ERα reached 79.9% in the control group. Compared to the control group, the number of KiSS1/ERα-dual

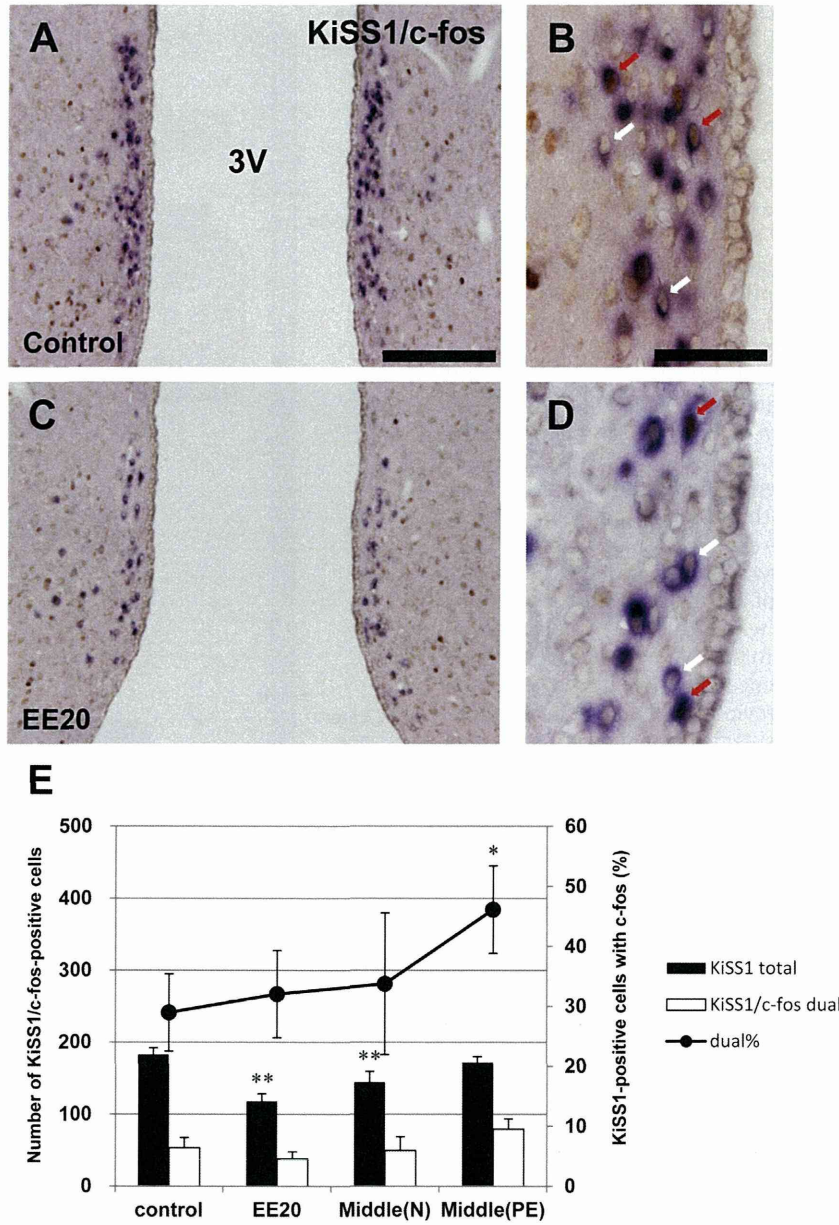

Fig. 7. Representative images of dual-labeling ISH/IHC for KiSS1/c-fos in the AVPV in control (A and B) and EE20 (C and D) groups. Most positive cells show dark blue cytoplasimic staining for KiSS1 mRNA and brown nuclear staining for c-fos. Red arrows represent KiSS1/c-fos-double positive cells and white arrows represent KiSS1 mRNA-single positive cells. Percentage of KiSS1-positive cells showing nuclear c-fos immunoreactivity was not changed in EE20 and Middle (N) groups, but significantly increased in Middle (PE) group (E). Graph shows the total number of KiSS1-positive cells (closed bar), the number of KiSS1/c-fos double positive cells (open bar) and percentage of KiSS1-positive cells showing c-fos co-expression (line chart). All brain samples were collected during the interval from 16:00 to 17:00. Data are presented as mean ± S.D. or mean + S.D. ($n = 4$/group). Symbols indicate significant difference from the control group (*: $p < 0.05$ and **: $p < 0.01$ by Dunnett's test, respectively). 3 V: third ventricle. Scale bars = 200 μm (A and C) or 50 μm (B and D).

positive cells was significantly decreased in EE20 and Middle (N) groups, and the percentage of KiSS1-positive cells with ERα expression was also significantly decreased to 66.8% and 66.1% in EE20 and Middle (N) groups, respectively (Fig. 6E). In dual staining with KiSS1 and c-fos, the number of KiSS1/c-fos-dual positive cells was not significantly changed in these groups, and the percentage of KiSS1-positive cells co-expressing c-fos were 28.9%, 32.0% and 33.7% in control, EE20 and middle (N) group, respectively. In contrast, the number of KiSS1/c-fos-dual positive cells in Middle (PE) group slightly increased, and the percentage of KiSS1-positive cells with c-fos expression was reached 46.1%, significantly increased compared to that of control group (Fig. 7E).

4. Discussion

Kisspeptin is one of the most recently discovered neuropeptides and is a central regulator of GnRH and gonadotropin secretion in the HPG axis, consequently controlling various reproductive functions, including estrous cycle, ovulation, and follicular development [17,18]. Kisspeptin plays a site-specific role in regulating ovulation by induction of preovulatory LH surges through positive feedback in the AVPV [24] and regulating folliculogenesis through pulsatile GnRH secretion in the ARC. In previous studies, we reported the early onset of age-related abnormal estrous cycles in neonatally EE-exposed rats [11], indicating some sort of disruption in neuroendocrine pathway. Thus, we investigated the changes in the LH

surge and KiSS1 mRNA expression in normally cycling young adult animals neonatally exposed to EE.

In the present study, real-time PCR analysis revealed that KiSS1 mRNA expression in the AVPV peaked at 16:00–17:00, the same time as the peak of LH surge in each group. This result indicates rapid transmission of kisspeptin and GnRH neuron, which results in quick gonadotropin secretion from the pituitary. In inter-group comparisons, KiSS1 mRNA expression in the AVPV at 14:00 was significantly decreased in the EE20 and Middle (N) groups, to nearly half the level of the control group, and the decreasing trend was maintained up to 16:00 in both groups. Furthermore, in the more site-specific analysis by ISH, we found that the number of KiSS1 mRNA-positive cells and their signal intensities in the AVPV were significantly decreased in the EE20 and Middle (N) groups. These results clearly indicate the down-regulation of KiSS1/GPR54 signaling and neurotransmission in the HPG axis at the time of the LH surge, suggesting the attenuation of the reactivity to exogenous estrogenic treatment in delayed effect and middle-aged animals. In addition, we also found that the number and percentage of KiSS1/ERα-dual positive cells were significantly decreased in these groups, possibly indicating that down-regulation of KiSS1 signaling might be related to the decrease of ERα expression. These results also mean that a single treatment with EE at PND 0 induces attenuation of KiSS1 mRNA expression in the AVPV even approximately 2 months earlier than the occurrence of early onset of abnormal estrous cycling reported in our previous study [11]. On the other hand, in the ARC, no statistically significant change was observed in KiSS1 mRNA expression at 16:00, and the number and intensity of KiSS1-positive cells were also not changed among control, EE-exposed, and middle-age groups. Therefore, it could be said that the attenuation of KiSS1 mRNA expression in the delayed effect and middle-aged rats was specific to the AVPV, and, thus, follicular development may not be influenced by the delayed effect.

Regarding other KiSS1-related genes, none of the investigated genes (KiSS1R, ERα, ERβ and c-fos) exhibited any significant differences in mRNA expression detected by quantitative real-time PCR. The discrepancy of ERα expression between real-time PCR and dual-labeling ISH/IHC might be due to abundant ERα expressing cells other than the kisspeptin neuron in the area surrounding 3V, thus the site-specific assay like a dual-labeling ISH/IHC is considered to be more robust technique for detection of common molecules in the kisspeptin neuron. In contrast, consistent with the results in real-time PCR, percentage of KiSS1-positive neuron with c-fos immunoreactivity was not changed in EE20 and Middle (N) groups. In previous studies, c-fos co-expression in kisspeptin neurons was clearly related to the functional activity of kisspeptin neurons and the following LH surge [20,23]. Recently, Ishii et al. [36] also reported that the percentage of KiSS1 mRNA-positive cells with c-fos immunoreactivity decreased in middle aged female rats. In these studies, percentage of c-fos co-expression in activated kisspeptin neuron reached nearly 60%. The precise reason is not determined, but the lower percentage of c-fos co-expression in our control group might contribute to this contradictory result. On the other hand, the percentage of KiSS1/c-fos-dual positive cells in Middle (PE) group significantly increased in our study, indicating the increased reactivity to estrogens in this group. This may result from the possible imbalance of feedback system in this acyclic group associated with the cessation of estrous cycle, but this hypothesis needs to be verified by further investigation.

Assay of serum LH concentrations in the control group indicated that the peak time of LH surge in the environment of our facility was at 16:00, although those of all EE-exposed groups were at 17:00. In addition, dose-related reduction of the LH peak area and peak concentration at 16:00 was observed in the EE20 and EE0.2 groups, and these decreases were more evident in the Middle (N) and (PE) groups, indicating reduced peak amplitude and delayed peak time

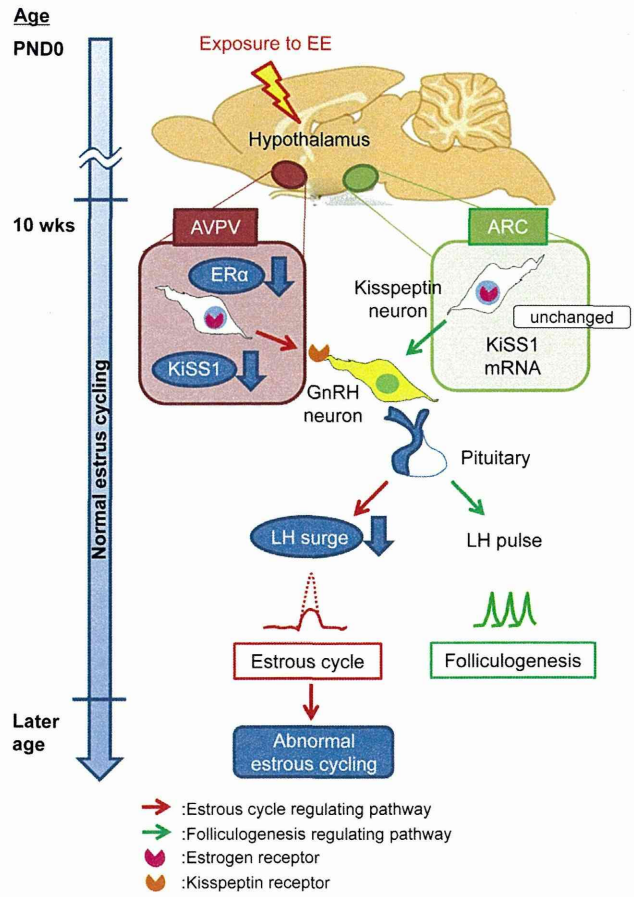

Fig. 8. Proposed pathway for the delayed effect. Neonatal exposure to EE induces an AVPV-specific decrease in KiSS1 and ERα mRNA expression and a consequent attenuation of LH surge in young adult rats, leading to the early onset of abnormal estrous cycling.

for the LH surge. Since activation of hypothalamic kisspeptin and GnRH neurons is essential for the induction of the preovulatory LH surge [23], it is highly possible that the depression in KiSS1 mRNA expression observed in the present study leads to these functional changes in the LH surge. The attenuation of LH surge could also contribute to the cessation of ovulation and early onset of abnormal estrous cycling in the delayed effect. The proposed pathway is shown in Fig. 8.

Attenuation and delay of the LH surge are normal senescence processes of the estrous cycle in middle-aged rats [37–39], and these changes associated with aging have also been reported to precede the cessation of regular estrous cycling [40]. Recently, moreover, not only the alteration in the LH surge, but also attenuation of KiSS1/GPR54 signaling in the hypothalamus of middle-aged rats have been reported in several articles [28,29,41], suggesting depression of kisspeptin neuron might be a trigger for age-related LH surge dysfunction and reproductive aging [28]. In the present study, we confirmed the similar serial dysfunction of the kisspeptin neuron and LH surge in young adult animals neonatally exposed to EE. Similar to reproductive aging and the delayed effect, high dose neonatal exposure to various estrogenic compounds such as bisphenol-A, 17alpha-ethynylestradiol, estradiol benzoate, and selective ERα agonists also showed attenuation of the LH surge [42,43], KiSS1 mRNA expression, and/or immunoreactivity for kisspeptin in the hypothalamic kisspeptin neurons [30–32].

Another important finding in the present study is the fact that all these hypothalamic and hormonal changes occurred before the onset of abnormal estrous cycling, indicating that the disruption

of KiSS1/GPR54 signaling is also an early key event in serial, late-occurring reproductive dysfunctions in the delayed effect. Recently, our laboratory also identified that the rat neonatally exposed to various dose of EE showed the decreased FSH levels at PND14 and decreased ERα expression in the uterine epithelium at 10 weeks of age [44]. These early stage functional changes in the kisspeptin neuron, hormone balance and reproductive tissues might have the possibility to be the useful indicator for the delayed effects substitute for the abnormal estrous cycle occurred in later age, and may provide a new clue for the further investigation and risk identification of the delayed effect induced by the estrogenic chemicals like EDCs.

Interestingly, several investigations that focused on the perinatal development of kisspeptin neurons have revealed that KiSS1 mRNA-positive cells in the AVPV are first detected at PND 12 and that kisspeptin-expressing neurons progressively increase approximately from PND 25–35 until puberty onset in the mouse brain [26,45]. These results have provoked controversy over the question of what the direct target of the neonatal exposure to xenobiotic compounds in the delayed effect may be. Thus, the underlying target of estrogen exposure in the neonatal period that induces the delayed effect needs to be further elucidated.

5. Conclusion

In conclusion, we found attenuation and a delayed peak in the LH surge and depression of KiSS1 mRNA expression in the AVPV in both neonatal EE-exposed and middle-aged rats. These AVPV-specific changes indicate the disruption of the LH surge center that consequently may cause the early onset of abnormal estrous cycling in the delayed effect. Since these changes were observed in both of delayed effect and aging animals, the delayed effect may be relevant to reproductive aging. Furthermore, in light of the earlier occurrence of hypothalamic and hormonal changes than in abnormal estrous cycling, attenuation of the LH surge and KiSS1 mRNA expression have the possibility of being early stage toxicological indicators of the delayed effect, may provide the new clue for the risk assessment of estrogenic chemicals like EDCs.

Conflict of interest

The first author is an employee of Mochida Pharmaceutical Co., Ltd., but there is no conflict of interest to be declared for this publication. The company and funding organizations do not have control over the resulting publication.

Transparency document

The Transparency document associated with this article can be found in the online version.

Acknowledgments

We thank Mss. Ayako Saikawa and Yoshimi Komatsu for expert technical assistance in processing histopathological sections. This work was supported by the Health and Labor Sciences Research Grants, Research on Risk of Chemical Substances, Ministry of Health, Labor and Welfare, Japan [H25-Toxicol-003].

References

[1] Diamanti-Kandarakis E, Bourguignon JP, Giudice LC, Hauser R, Prins GS, Soto AM, et al. Endocrine-disrupting chemicals: an Endocrine Society scientific statement. Endocr Rev 2009;30:293–342.
[2] Jeung EB, Choi KC. Toxicological mechanism of endocrine disrupting chemicals: is estrogen receptor involved? Toxicol Res 2010;26:237–43.
[3] Markey CM, Rubin BS, Soto AM, Sonnenschein C. Endocrine disruptors: from Wingspread to environmental developmental biology. J Steroid Biochem Mol Biol 2002;83:235–44.
[4] Newbold RR. Developmental exposure to endocrine-disrupting chemicals programs for reproductive tract alterations and obesity later in life. Am J Clin Nutr 2011;94:1939S–42S.
[5] Christensen LW, Gorski RA. Independent masculinization of neuroendocrine systems by intracerebral implants of testosterone or estradiol in the neonatal female rat. Brain Res 1978;146:325–40.
[6] Katsuda S, Yoshida M, Watanabe G, Taya K, Maekawa A. Irreversible effects of neonatal exposure to *p*-tert-octylphenol on the reproductive tract in female rats. Toxicol Appl Pharmacol 2000;165:217–26.
[7] McLachlan JA, Newbold RR, Shah HC, Hogan MD, Dixon RL. Reduced fertility in female mice exposed transplacentally to diethylstilbestrol (DES). Fertil Steril 1982;38:364–71.
[8] Yoshida M, Katsuda S, Tanimoto T, Asai S, Nakae D, Kurokawa Y, et al. Induction of different types of uterine adenocarcinomas in Donryu rats due to neonatal exposure to high-dose *p*-t-octylphenol for different periods. Carcinogenesis 2002;23:1745–50.
[9] Gore AC, Walker DM, Zama AM, Armenti AE, Uzumcu M. Early life exposure to endocrine-disrupting chemicals causes lifelong molecular reprogramming of the hypothalamus and premature reproductive aging. Mol Endocrinol 2011;25:2157–68.
[10] Yoshida M, Takahashi M, Inoue K, Hayashi S, Maekawa A, Nishikawa A. Delayed adverse effects of neonatal exposure to diethylstilbestrol and their dose dependency in female rats. Toxicol Pathol 2011;39:823–34.
[11] Takahashi M, Inoue K, Morikawa T, Matsuo S, Hayashi S, Tamura K, et al. Delayed effects of neonatal exposure to 17alpha-ethynylestradiol on the estrous cycle and uterine carcinogenesis in Wistar Hannover GALAS rats. Reprod Toxicol 2013;40:16–23.
[12] Shiorta M, Kawashima J, Nakamura T, Ogawa Y, Kamiie J, Yasuno K, et al. Delayed effects of single neonatal subcutaneous exposure of low-dose 17α-ethynylestradiol on reproductive function in female rats. J Toxicol Sci 2012;37:681–90.
[13] Ohta R, Ohmukai H, Marumo H, Shindo T, Nagata T, Ono H. Delayed reproductive dysfunction in female rats induced by early life exposure to low-dose diethylstilbestrol. Reprod Toxicol 2012;34:323–30.
[14] Kotani M, Detheux M, Vandenbogaerde A, Communi D, Vanderwinden JM, Le Poul E, et al. The metastasis suppressor gene KiSS-1 encodes kisspeptins, the natural ligands of the orphan G protein-coupled receptor GPR54. J Biol Chem 2001;276:34631–6.
[15] Ohtaki T, Shintani Y, Honda S, Matsumoto H, Hori A, Kanehashi K, et al. Metastasis suppressor gene KiSS-1 encodes peptide ligand of a G-protein-coupled receptor. Nature 2001;411:613–7.
[16] Smith JT, Clifton DK, Steiner RA. Regulation of the neuroendocrine reproductive axis by kisspeptin-GPR54 signaling. Reproduction 2006;131:623–30.
[17] Kauffman AS, Clifton DK, Steiner RA. Emerging ideas about kisspeptin-GPR54 signaling in the neuroendocrine regulation of reproduction. Trends Neurosci 2007;30:504–11.
[18] Maeda K, Adachi S, Inoue K, Ohkura S, Tsukamura H. Metastin/kisspeptin and control of estrous cycle in rats. Rev Endocr Metab Disord 2007;8:21–9.
[19] Dungan HM, Clifton DK, Steiner RA. Minireview: kisspeptin neurons as central processors in the regulation of gonadotropin-releasing hormone secretion. Endocrinology 2006;147:1154–8.
[20] Adachi S, Yamada S, Takatsu Y, Matsui H, Kinoshita M, Takase K, et al. Involvement of anteroventral periventricular metastin/kisspeptin neurons in estrogen positive feedback action on luteinizing hormone release in female rats. J Reprod Dev 2007;53:367–78.
[21] Smith JT. Kisspeptin signalling in the brain: steroid regulation in the rodent and ewe. Brain Res Rev 2008;57:288–98.
[22] García-Galiano D, Pinilla L, Tena-Sempere M. Sex steroids and the control of the Kiss1 system: developmental roles and major regulatory actions. J Neuroendocrinol 2012;24:22–33.
[23] Clarkson J, d'Anglemont de Tassigny X, Moreno AS, Colledge WH, Herbison AE. Kisspeptin-GPR54 signaling is essential for preovulatory gonadotropin-releasing hormone neuron activation and the luteinizing hormone surge. J Neurosci 2008;28:8691–7.
[24] Colledge WH. GPR54 and kisspeptins. Results Probl Cell Differ 2008;46:117–43.
[25] Irwig MS, Fraley GS, Smith JT, Acohido BV, Popa SM, Cunningham MJ, et al. Kisspeptin activation of gonadotropin releasing hormone neurons and regulation of KiSS-1 mRNA in the male rat. Neuroendocrinology 2004;80:264–72.
[26] Clarkson J, Herbison AE. Postnatal development of kisspeptin neurons in mouse hypothalamus; sexual dimorphism and projections to gonadotropin-releasing hormone neurons. Endocrinology 2006;147:5817–25.
[27] Kauffman AS, Gottsch ML, Roa J, Byquist AC, Crown A, Clifton DK, et al. Sexual differentiation of Kiss1 gene expression in the brain of the rat. Endocrinology 2007;148:1774–83.
[28] Lederman MA, Lebesgue D, Gonzalez VV, Shu J, Merhi ZO, Etgen AM, et al. Age-related LH surge dysfunction correlates with reduced responsiveness of hypothalamic anteroventral periventricular nucleus kisspeptin neurons to estradiol positive feedback in middle-aged rats. Neuropharmacology 2010;58:314–20.
[29] Neal-Perry G, Lebesgue D, Lederman M, Shu J, Zeevalk GD, Etgen AM. The excitatory peptide kisspeptin restores the luteinizing hormone surge and modulates amino acid neurotransmission in the medial preoptic area of middle-aged rats. Endocrinology 2009;150:3699–708.

[30] Bateman HL, Patisaul HB. Disrupted female reproductive physiology following neonatal exposure to phytoestrogens or estrogen specific ligands is associated with decreased GnRH activation and kisspeptin fiber density in the hypothalamus. Neurotoxicology 2008;29:988–97.
[31] Navarro VM, Sánchez-Garrido MA, Castellano JM, Roa J, García-Galiano D, Pineda R, et al. Persistent impairment of hypothalamic KiSS-1 system after exposures to estrogenic compounds at critical periods of brain sex differentiation. Endocrinology 2009;150:2359–67.
[32] Patisaul HB, Todd KL, Mickens JA, Adewale HB. Impact of neonatal exposure to the ERalpha agonist PPT, bisphenol-A or phytoestrogens on hypothalamic kisspeptin fiber density in male and female rats. Neurotoxicology 2009; 30:350–7.
[33] Düsterberg B, Kühne G, Täuber U. Half-lives in plasma and bioavailability of ethinylestradiol in laboratory animals. Arzneimittelforschung 1986;36: 1187–90.
[34] Navarro VM, Castellano JM, Fernández-Fernández R, Barreiro ML, Roa J, Sanchez-Criado JE, et al. Developmental and hormonally regulated messenger ribonucleic acid expression of KiSS-1 and its putative receptor, GPR54, in rat hypothalamus and potent luteinizing hormone-releasing activity of KiSS-1 peptide. Endocrinology 2004;145:4565–74.
[35] Taya K, Mizokawa T, Matsui T, Sasamoto S. Induction of superovulation in prepubertal female rats by anterior pituitary transplants. J Reprod Fertil 1983;69:265–70.
[36] Ishii MN, Matsumoto K, Matsui H, Seki N, Matsumoto H, Ishikawa K, et al. Reduced responsiveness of kisspeptin neurons to estrogenic positive feedback associated with age-related disappearance of LH surge in middle-age female rats. Gen Comp Endocrinol 2013;193:121–9.
[37] Cooper RL, Roberts B, Rogers DC, Seay SG, Conn PM. Endocrine status versus chronologic age as predictors of altered luteinizing hormone secretion in the "aging" rat. Endocrinology 1984;114:391–6.
[38] DePaolo LV, Chappel SC. Alterations in the secretion and production of follicle-stimulating hormone precede age-related lengthening of estrous cycles in rats. Endocrinology 1986;118:1127–33.
[39] Wise PM. Alterations in the proestrous pattern of median eminence LHRH, serum LH, FSH, estradiol and progesterone concentrations in middle-aged rats. Life Sci 1982;31:165–73.
[40] Nass TE, LaPolt PS, Judd HL, Lu JK. Alterations in ovarian steroid and gonadotrophin secretion preceding the cessation of regular oestrous cycles in ageing female rats. J Endocrinol 1984;100:43–50.
[41] Zhang J, Yang L, Lin N, Pan X, Zhu Y, Chen X. Aging-related changes in RP3V kisspeptin neurons predate the reduced activation of GnRH neurons during the early reproductive decline in female mice. Neurobiol Aging 2014;35: 655–68.
[42] Herath CB, Watanabe G, Katsuda S, Yoshida M, Suzuki AK, Taya K. Exposure of neonatal female rats to *p*-tert-octylphenol disrupts afternoon surges of luteinizing hormone, follicle-stimulating hormone and prolactin secretion, and interferes with sexual receptive behavior in adulthood. Biol Reprod 2001;64:1216–24.
[43] Nozawa K, Nagaoka K, Zhang H, Usuda K, Okazaki S, Taya K, et al. Neonatal exposure to 17α-ethynyl estradiol affects ovarian gene expression and disrupts reproductive cycles in female rats. Reprod Toxicol 2014;46:77–84.
[44] Takahashi M, Inoue K, Morikawa T, Matsuo S, Hayashi S, Tamura K, et al. Early indicators of delayed adverse effects in female reproductive organs in rats receiving neonatal exposure to 17alpha-ethynylestradiol. J Toxicol Sci 2014;39:775–84.
[45] Knoll JG, Clay CM, Bouma GJ, Henion TR, Schwarting GA, Millar RP, et al. Developmental profile and sexually dimorphic expression of kiss1 and kiss1r in the fetal mouse brain. Front Endocrinol (Lausanne) 2013;4:140.

Reproductive Toxicology 57 (2015) 21–28

Contents lists available at ScienceDirect

Reproductive Toxicology

journal homepage: www.elsevier.com/locate/reprotox

Predominant role of the hypothalamic–pituitary axis, not the ovary, in different types of abnormal cycle induction by postnatal exposure to high dose *p-tert*-octylphenol in rats

Midori Yoshida[a,*], Sayumi Katashima[b], Miwa Tahahashi[a], Ryohei Ichimura[a,b], Kaoru Inoue[a], Kazuyoshi Taya[b], Gen Watanabe[b]

[a] *Division of Pathology, National Institute of Health Sciences, 1-18-1, Kamiyoga, Setagaya-ku, Tokyo 158-8501, Japan*
[b] *Veterinary Physiology, Tokyo University of Agriculture and Technology, 3-5-8, Saiwaicho, Fuchu-shi, 183-8509 Tokyo, Japan*

ARTICLE INFO

Article history:
Received 9 April 2014
Received in revised form 31 March 2015
Accepted 1 May 2015
Available online 11 May 2015

Keywords:
Delayed effect
Estrous cycle
Hypothalamic–pituitary axis
Ovary exchange
Postnatal exposure
p-tert-Octylphenol

ABSTRACT

To determine whether it is the hypothalamic–pituitary axis or the ovary that plays the predominant role in abnormal estrous cycling induction by postnatal exposure to estrogenic compounds, female rats were subcutaneously injected with 100 mg/kg *p-tert*-octylphenol or vehicle for 5 or 15 days after birth (OP-PND5, OP-PND15 or control). Ovaries were exchanged between control and treated groups on PND28. Controls receiving control or OP-PND5 ovaries showed normal cycles within 4 weeks after the exchange, and corpora lutea were detected in transplanted ovaries. Controls receiving OP-PND15 ovaries consistently increased persistent estrus (PE). OP-PND15 rats receiving control or OP-PND15 ovaries immediately descended into PE, and transplanted ovaries were atrophic with cystic follicles, indicating anovulation. OP-PND5 rats receiving control or OP-PND5 ovaries showed early onset of PE after normal cycling. The hypothalamic–pituitary axis is predominant in abnormal cycling induction by postnatal exposure to OP. OP-PND15 ovaries were impaired compared to other groups.

1. Introduction

Perinatal exposure to estrogenic compounds has the potential to induce functionally and/or structurally irreversible effects on the reproductive tract in both rodents and humans [1,2]. Perinatal exposure to steroid hormones during critical periods is well known to induce defeminization in females [3], characterized by low gonadotropin levels at prepuberty, anovulation resulting in atrophic ovary, and persistent estrus (PE) [4–6]. As for other perinatal effects, decreased uterine gland genesis and abnormal expression of uterine estrogen receptors have been reported in rodents [7–10]. All of these effects are manifested before puberty or in young adulthood. When these effects occur early in life, they lead to the increase the risk of vaginal cancer in women [1] and cervical and uterine cancer in rats and mice [11–13].

The perinatal effects of shorter or lower-dose exposure to estrogenic compounds have also been reported to induce delayed-type changes that differ from the typical effects of defeminization described above. The delayed-type postnatal effect has not been well investigated, but early onset of aged-matched abnormal cycling has been accepted as a common feature of the adverse effect elicited after maturation [14,15]. Recently, the issue of endocrine disruption has again been addressed in the endocrinology and toxicology fields [16,17], and new studies have addressed the delayed adverse effect of perinatal exposure to estrogen using various endpoints [18–22]. In our previous report on the delayed adverse effect of neonatal exposure to various doses of 17α-estradiol (EE) in rats, the most sensitive endpoint for the delayed effect was an early onset of age-matched abnormal estrous cycling with a clear dose dependence. The timing of appearance at the lowest effective dose – 0.2 μg/kg bw – was 22 weeks after birth [20]. As for other endpoints for delayed adverse effect, increased uterine and mammary cancer risks have been reported [13,23]. These risks are linked to early occurrence of PE and/or ovarian atrophy with lack of corpora lutea (CL), suggesting that they might be secondary effects due to a prolonged increase in relative estrogen levels. Therefore, clarification of the delayed adverse effect is

Abbreviations: bw, body weight; EE, 17alpha-estradiol; OP, *p-tert*-octylphenol; PND, postnatal day; PE, persistent estrus.

* Corresponding author. Tel.: +81 3 3700 9821; fax: +81 3 3700 1425.
E-mail address: midoriy@nihs.go.jp (M. Yoshida).

http://dx.doi.org/10.1016/j.reprotox.2015.05.001
0890-6238/

needed for a better understanding of the mechanisms of perinatal exposure to estrogens and endocrine disruptors with estrogenic activity.

The estrous cycle is controlled by the hypothalamo–pituitary–gonadal (HPG) system. In particular, the anterior part of the hypothalamic plays an essential role as the LH surge control center in mammals. Defeminization of rats induced by exposure to estrogens or androgens during critical periods is known to result from the disruption of hypothalamic function and the resulting decrease in gonadotropin levels and onset of anovulation [6,24], but effects on the ovary remain to be fully determined. Abnormal cyclicity is a common feature of senescence in mammals; however, the pathway most responsible for abnormal cyclicity in rodents has been reported to be different from that in humans. Naturally occurring abnormal cycles, including PE, in middle-aged rats are accepted as a feature of rodent reproductive senescence. The aging hypothalamic–pituitary axis in rodents, unlike the one in primates, directly contributes to reproductive senescence [25]. In contrast, senescence in the ovary has been reported to play a crucial role in menopause in women [26–28]; however, aging in the HPG axis system has been reported to be independent of the changes in the ovarian hormonal milieu of the menopausal transition [28].

p-tert octylphenol (OP), an alkylphenol, is derived from biodegradation of nonionic surfactants used for detergents in industry and had found in the sludge of sewage-treatment plants, as well as in river sediments, although the estimated level of harm in environmental concentrations including fresh water and seawater were getting much lower, and were not concern levels for more information in 2011 in Japan (http://www.env.go.jp/chemi/report/h21-01/index.html). OP has estrogenic activity at high doses [29–32]. The estrogenic activity of OP has been measured in vivo using a uterotropic assay in which OP was subcutaneously injected at a dose of 25 mg/kg bw or higher (equivalent to 80 ng/ml in serum) in rats [30]. Postnatal exposure to high doses of OP (subcutaneous injection of 100 mg/kg bw every other day from postnatal day (PND) 1–15) had defeminizing effects similar to those of xenobiotics with estrogenic activity, such as lower gonadotropin levels before puberty, anovulation leading to persistent estrus, abnormal estrogen receptor α expression, and induction of endometrial adenocarcinomas with increased malignancy [6,10]. In our previous study, shorter-term neonatal exposure to the same dose of OP (subcutaneous injection of 100 mg/kg bw on PNDs 1, 3, and 5) induced early onset of age-matched PE without apparent adverse effects up to young adulthood, suggesting that the shorter-term neonatal treatment with OP could induce delayed adverse effects [13]. In addition, the shorter-term treatment increased the incidence of well-differentiated endometrial adenocarcinoma, a common type of tumor in the rat strain examined. Whereas the delayed-type effects are considered adverse to females due to concern over reduced fertility related to early onset of abnormal cycling and increased risk of uterine cancer, the mechanism of the delayed-type effect has not been determined. In addition, delayed adverse effects on ovulation and reproduction have not been reported.

The present study used ovary exchange to determine whether it is the hypothalamic–pituitary axis or the ovary that is the primary mediator of induction of abnormal estrous cycle both in the delayed effect and defeminization in rats postnatally exposed to OP, estrogenic compounds. In addition, delayed adverse effects of neonatal exposure to OP on ovulation at estrus morning and on reproductive abilities were also evaluated. We chose OP as the estrogenic compound because the dose–duration relationship between this compound and the delayed effect has already been reported.

2. Materials and methods

2.1. Animals and housing conditions

Twenty-three pregnant female Crj:Donryu rats were purchased from Charles River Japan, Inc. (Kanagawa, Japan). Pregnant dams and dams with offspring were housed in plastic cages until pups reached PND 21, the weaning age. The day of birth was designated PND 0. To obtain as many female offspring as possible, all female pups were kept, and litter sizes were adjusted to 10/dam at PND 4. After weaning at PND 21, the females were segregated from the males. All female offspring were used in the present study, and 20 male offspring obtained from the control group were stocked for mating in experiment 3 (see below). The remaining males were euthanized at weaning. Female rats were housed four per cage in the same treatment groups and maintained until termination. Males were housed three per cage. Animals were kept in an air-controlled animal room under constant conditions of 24 ± 2 °C and 55 ± 10% humidity with a 12-h light/dark cycle and maintained on basal diet CRF-1 (Oriental Yeast, Inc., Tokyo, Japan) and tap water *ad libitum*. Animal experimental protocols were reviewed and approved by the animal ethical committee of Sasaki Institute (Tokyo, Japan), where all animal studies were conducted.

2.2. Chemicals and treatment

2.2.1. Chemicals

OP (Wako Pure Chemical, Osaka, Japan) was dissolved in dimethyl sulfoxide (purity 99.9%; DMSO, Wako Pure Chemical, Osaka, Japan). Dosing volume was 0.5 ml/100 g body weight.

2.2.2. Treatment

OP was delivered subcutaneously at 100 mg/kg bw/day on PND1 (within 24 h after birth), 3, 5, 7, 9, 11, 13, and 15 (OP-PND15) for induction of defeminization, and on PND1, 3, and 5 (OP-PND5) for induction of the delayed adverse effect characterized by early onset of PE. Control rats were given subcutaneous injections of vehicle (DMSO) only. To avoid contamination during allocation of female offspring, 23 dams were divided into three groups (10 dams for control group, 8 dams for OP-PND5 and 5 dams for OP-PND15 groups) before treatment of female offspring. The dose and dosing schedules were chosen based on our previous studies [6,13]. Briefly, our previous studies indicated that: (1) subcutaneous treatment with 100 mg/kg bw of OP had estrogenic activity, (2) OP-PND15 induced low gonadotropin levels at prepuberty and anovulation resulting in atrophic ovary, or PE immediately after puberty, which are typical indicators of defeminization, and (3) OP-PND5 induced early onset of age-matched abnormal cycle (mainly PE) in our previous study.

The total number of female offspring examined was 125, which were divided into 58, 42, and 25 for the control, OP-PND5, and OP-PND15 groups, respectively. Allocation and numbers of female rats used in the following three experiments are shown in Table 1. The designs of the three experiments are shown in Fig. 1. To eliminate potential litter effects, female offspring were selected from different dams in each group as much as possible (Table 1).

2.3. Ovary exchange (experiment 1)

To determine whether it is the hypothalamic–pituitary axis or the ovary that plays the predominant role in mediating induction of defeminization and the delayed adverse effect upon postnatal exposure to OP, ovaries were exchanged. Female rats in the control (24 rats), OP-PND5 (17 rats), and OP-PND15 (14 rats) groups were bilaterally ovariectomized on PND28 under anesthesia. The paired ovaries were removed and transplanted into the back subcutis of different animals in the same or other groups (Table 1). The rats

Table 1
Allocation and numbers of female rats examined.

Group	Control	OP-PND5	OP-PND15
Total number of females used in Exps. 1–3	58 (10)	42 (8)	25 (5)
Number of rats used for ovarian change (Exp. 1)	22 (10)	17 (8)	14 (5)
Number of rats ovariectomized	24 (10)	17 (8)	14 (5)
Rats receiving ovaries from control group	6 (6)[a]	10 (9)	7 (5)
Rats receiving ovaries from OP-PND5 group	9 (9)[a]	7 (7)	NE
Rats receiving ovaries from OP-PND15 group	7 (7)	NE	7 (5)
Number of paired ovaries donated	24 (10)	17 (8)	14 (5)
Ovaries donated to control group	7 (6)	10 (9)	7 (7)
Ovaries donated to OP-PND5 group	10 (9)	7 (7)	NE
Ovaries donated to OP-PND15 group	7 (7)	NE	7(5)
Number of rats without surgical operation	36 (10)	25 (8)	11 (5)
Number of rats monitored for cycling only up to terminal sacrifice	20	2	3
Exp. 2			
Number of rats used for counting follicles	8	15	8
Exp. 3			
Number of rats used for reproduction ability	8	8	NE

[a] Two females (in the control groups receiving ovaries from a control group rat and from an OP-PND5 group rat) had failed ovariectomies and were excluded from Exp. 1.
NE, not examined.
Numbers in parentheses indicate number of dams delivering females used in Exps. 1–3.

in the control group were subdivided into three groups, receiving ovaries from control (6 rats), OP-PND 5 (9 rats), and OP-PND15 (7 rats) groups. Two females (one receiving ovaries from the control and one from the OP-PND5 group) had failed ovariectomies and were excluded. The rats in the OP-PND5 group were subdivided into two groups, receiving ovaries from control (10 rats) and OP-PND5 (7 rats) groups, and the rats in the OP-PND15 group were subdivided into 2 groups, receiving ovaries from control (7 rats) and OP-PND15 (7 rats) groups.

Ovariectomies were conducted by veterinarians, with an average time for surgery under 5 min per rat. After surgery, animals were maintained in plastic cages with fresh wooden chips and carefully monitored by the veterinarians until recovery. All animals woke up within 10 min after surgery and completely recovered normal behavior, including grooming, eating, and drinking, by the evening.

Estrous cycle was monitored in all rats beginning 1 week after ovary exchange (at 5 weeks of age) and continuing throughout the duration of the study. Ovary-exchanged rats were compared both within and between groups to identify differences. In addition, estrous cycles of rats receiving ovaries were compared with those of rats that did not undergo surgery (36, 25, and 11 rats at the beginning in the control, OP-PND5, and OP-PND15 group, respectively). The remaining rats without transplanted ovaries in the OP-PND5 and OP-PND15 groups were monitored up to termination, but their estrous cyclicity was not tabulated after 14 weeks of age because the number of rats was too small for statistical analysis.

All animals receiving ovaries were euthanized under deep anesthesia at 16 or 17 weeks of age (12 or 13 weeks after ovary exchange). At termination, donated ovaries in the back subcutis were dissected out and fixed in neutral buffered formaldehyde solution. All brains, pituitary glands, adrenals, uteri, and vaginae

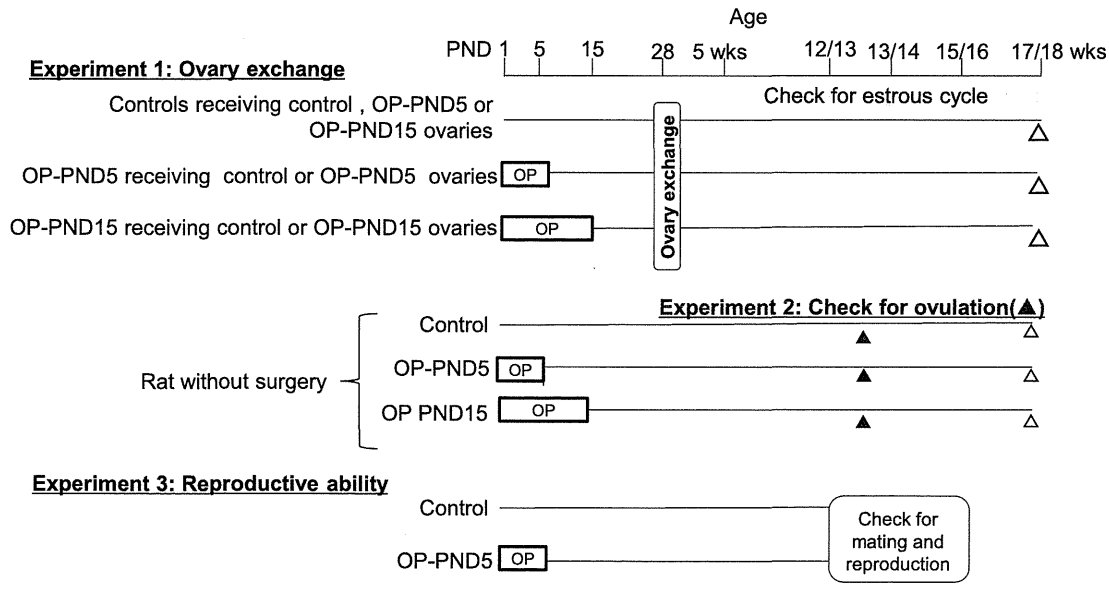

Fig. 1. Experimental design for the present study. PND, postnatal day; wks, weeks of age; OP-PND5, subcutaneous treatment with *t-tert*-octylphenol (OP) on PND1, 3, and 5; OP-PND15, subcutaneous treatment with OP on PND1, 3, 5, 7, 9, 11, 13 and 15; △, necropsy.

from these animals were also fixed. The same organs/tissues in the rats without surgery were also fixed. These organs/tissues were processed by routine methods and stained with hematoxylin and eosin for histological examination. Morphological classification of the corpora lutea (CL) was performed in accordance with the female reproductive tract group of INHAND (go RENI, http://www.goreni.org/). Briefly, the most recent CL indicate new CL formed within one cycle from the most current ovulation. Recent CL having a large size are formed before four or five cycles from the latest ovulation. Old CL are small ones with fibrosis or advanced regression of luteal cells.

2.4. Quantification of oocytes at ovulation (experiment 2)

Experiment 2 examined the effect of postnatal treatment with OP on ovulation. The animals were obtained from rats with intact ovaries in Exp. 1. At 13 or 14 weeks of age, the rats from the control (8 rats) and OP-PND5 (7 rats) groups showing normal cyclicity were euthanized on the morning of estrus under deep anesthesia, and ovaries and oviducts were bilaterally removed and placed in saline. The number of unstained oocytes obtained from each oviduct in the saline was counted under a microscope. Rats with irregular or persistent estrus in the OP-PND 5 (7 rats) and OP-PND15 (8 rats) groups were euthanized, and their oviducts were examined in the same manner.

2.5. Reproductive ability (experiment 3)

Experiment 3 examined reproductive ability in rats exposed to the delayed effect-inducing dose of OP postnatally. At 12 or 13 weeks of age, the cycling rats showing proestrus in the control and OP-PND 5 groups (8 females per group) were mated with intact males. Mating of females to littermates was avoided. The day on which sperm was detected in the vagina was designated gestation day 0. At gestation day 21, all females that had mated were euthanized under deep anesthesia and checked for the following parameters: litter size, body weights of pups (combined males and females), number of CL, number of implantation sites, and relative ovarian weight (mg/g bw). Ratios of number of implantation sites to CL and of litter size to number of implantation sites were calculated.

2.6. Statistical analysis

Data are expressed as mean values with standard deviation (SD). Differences among the control, OP-PND5, and OP-PND15 groups were assessed by the two-tailed *t*-test. The incidence of outcomes such as estrous cyclicity was analyzed using Fisher's exact test at $p > 0.05$. First, estrous cycles were compared using following three dimensions: First, intra-group differences were evaluated. The incidence of rats receiving ovaries from the control group was compared to those in rats receiving ovaries from the OP-PND5 and/or OP-PND15 groups in the same treatment group, and the significant differences were indicated by the symbol * in Fig. 2. Second, the incidences were compared for inter-group differences between rats in the control group receiving ovaries from the same group and the rats in the OP-PND5 and OP-PND15 groups, indicated by the symbol # in Fig. 2. Third, the differences between rats with and without ovarian exchange surgery were compared within the same treatment group, indicated by the symbol § in Fig. 2.

3. Results

3.1. Observations of live animals

The body weight gains among control and treatment groups with or without ovary exchange during the experimental period were similar. No treatment-related clinical signs were observed in either the ovary-exchange or intact groups.

3.2. Estrous cyclicity

The control rats receiving ovaries from control and OP-PND5 rats showed abnormal cycling during the first 2 weeks, but returned to normal cycling 3 weeks after surgical operation of ovary exchange (Fig. 2). Their cycling started to become irregular 12 weeks after the exchange (16 weeks of age). This change was similar to that of the control rats without surgery (left column in Fig. 2). In the control rats receiving ovaries from OP-PND15 rats, it took 2 weeks longer than for rats receiving ovaries from the control and OP-PND5 groups to show normal cycling after exchange. Although there was no statistically significant intra-group difference, the number of rats exhibiting PE increased in rats receiving OP-PND15 ovaries compared to rats receiving control and OP-PND5 ovaries in the control group (left column in Fig. 2). In comparison to rats in the corresponding control group without surgery, the number of control rats with ovaries from OP-PND15 rats that exhibited PE and/or irregular cycling was consistently high throughout most of the experimental period.

The operated OP-PND5 rats showed recovery in a sense that approximately 60% and higher of rats returned to normal cycling but not all of them. At 4 weeks after the operation, most of the rats showed normal cycling. The normal cyclicity in these rats changed to persistent estrus (PE) or irregular cycling at 5 or 7 weeks after the exchange (9 or 11 weeks of age). Most rats exhibited PE or an irregular cycle at the termination of the experiment. This magnitude was similar to that of the OP-PND5 rats without surgery up to 13 weeks of age (center column in Fig. 2).

Most rats in the PND15 group that received ovaries from the control or OP-PND15 group developed PE or an irregular cycle in their vaginal cytology within a few weeks, and all rats were affected by PE within 5 weeks after the exchange (9 weeks of age). The OP-PND15 rats without surgery also developed PE at an age similar to those of OP-PND15 rats receiving ovaries (right column in Fig. 2).

In comparisons of estrous cycling among the control, OP-PND5, and OP-PND15 groups without surgery, the regular cyclicity in the control group started to be abnormal cycling at 16 weeks of age. This age was similar to that reported in this strain rat [13,22]. The number of rats showing abnormal cycling was statistically increased in the OP-PND5 group starting at 12 weeks of age. This age is similar to that at which rats treated with OP-PND5 began to show abnormal cycling in our previous study [13]. All rats showed PE by 9 weeks of age in the OP-PND15 group; the timing of PE was similar to that observed in our previous study of OP [13].

3.3. Histology of implanted ovaries and other tissues

Representative histological sections of the implanted ovaries shown in Fig. 3, and a summary of the histology of the donated ovaries is shown in Table 2. In the control group rats receiving ovaries, abundant CL and various types of secondary follicles, including preantral or antral follicles, were detected in most ovaries transplanted from the control and OP-PND 5 groups into recipient subcutis (Fig. 3A). Primary follicles were also scattered. Large CL in the implanted ovaries were morphologically similar to the most recent or new CL detected in intact ovaries at each estrous stage. The presence of most recent CL indicates new CL formation after ovulation and the occurrence of ovulation within one estrous cycle stage. Most recent CL were found in approximately half of the transplanted ovaries donated from the control and OP-PND5 groups. Large antral follicles, which were similar to pre-ovulatory follicles, were also noted in the implanted ovaries of several rats

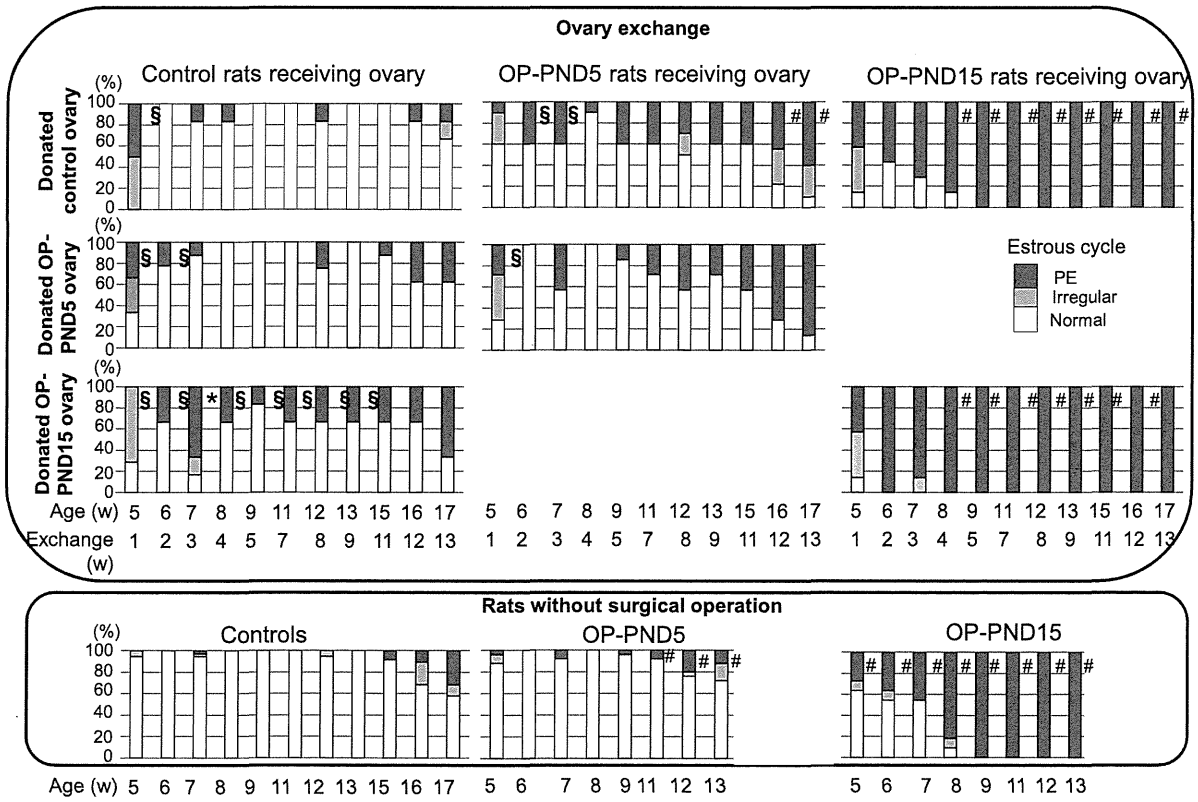

Fig. 2. Change in estrous cycling. Exchange (w), weeks after ovary exchange. In ovary exchange groups (circled by upper rectangle), left column is control rats receiving ovaries from control (upper), OP-PND5 (middle), and OP-PND15 (lower) groups. Center column is OP-PND5 group rats receiving ovaries from control (upper) and OP-PND5 (middle) groups. Right column is OP-PND15 group rats receiving ovaries from control (upper) and OP-PND15 (lower) groups. The bottom column indicates estrous cycling in the rats without surgery in the control (left), OP-PND5 (center), and OP-PND15 (right) groups (circled by lower rectangle). *Statistically significant intra-group differences between rats receiving OP-PND5 or OP-PND15 ovaries and those receiving control ovaries at $p < 0.05$ (Fischer's exact test). #Statistically significant inter-group differences between control, OP-PND5, and OP-PND15 groups receiving ovaries from the same group at $p < 0.05$ (Fischer's exact test). Statistically significant difference between ovary exchange groups and the no surgery group within the same treatment group at $p < 0.05$ (Fischer's exact test).

in the control group. In addition, histology in the ovary, uterus, and vagina, including vaginal smears from these rats, had the features of proestrus. Their typical histology was most recent CL of the proestrus type characterized as large, degenerating CL in the implanted ovaries (Fig. 3C), dilated and hydropic uterine horns, and cornified vaginal mucosa covering mucinous epithelium on the surfaces (Fig. 3D and insert). In the implanted ovaries from the OP-PND15 group, the number of most recent CL was lower than that from the control and OP-PND5 groups. Recent and/or old CL were observed in most ovaries transplanted from all groups to control group rats.

In the OP-PND5 group, there were no histological differences between the ovaries transplanted from the control and OP-PND5 groups. Most of the rats in the OP-PND5 group had ovaries with many recent and old CL. These histological findings were similar to those for the control group described above (Fig. 3B). One rat each receiving control and OP-PND5 ovaries had ovaries with most recent CL, a typical regular estrous cyclicity-related finding. There were no ovaries with pre-ovulatory follicles in the OP-PND5 group. In addition, several implanted ovaries lacked CL and had a few cystic atretic follicles, a typical histologic finding in ovaries after anovulation.

In the OP-PND5 group, the histological features of the ovaries transplanted from the control and OP-PND15 groups were comparable. Their findings were cystic atretic follicles and a few old CL (Fig. 3E), and this pattern was similar to that in the corresponding group of rats without surgery (Fig. 3F) and of ovaries after anovulation.

Table 2
Summary of histology in the donated ovaries.

Group		No. of rats examined	CL			Follicles		
Recipient	Donor		Most recent	Recent	Old	Secondary	Pre-ovulatory	Cystic
Control	Control	6	3[a]	4	6	6	1	0
	OP-PND5	9	5	7	9	9	1	0
	OP-PND15	7	2	3	6	4	0	0
OP-PND5	Control	10	1	2	7	10	0	3
	OP-PND5	7	1	4	3	7	0	5
OP-PND15	Control	7	0	0	3	7	0	6
	OP-PND15	7	0	0	2	6	0	6

[a] The number indicates the number of animals showing the histological feature in the donated ovaries.

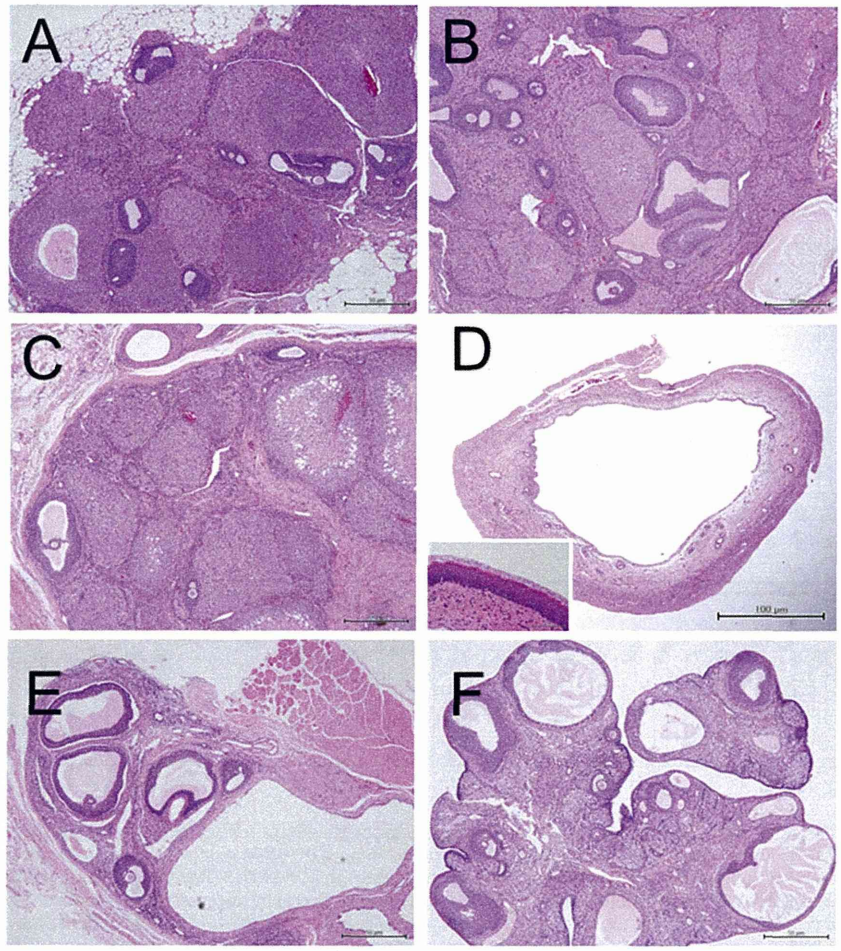

Fig. 3. Histology of ovaries implanted in the back subcutis at termination. (A) OP-PND5 ovary implanted in a control rat. (B) OP-PND5 ovary implanted in an OP-PND5 rat. (C) OP-PND5 ovary implanted in a control rat. (D) Uterus and vagina (insert) of the same rat as (C). (E) OP-PND15 ovary implanted in an OP-PND15 rat. (F) Ovary of rat without surgery in the OP-PND15 group. (A) and (B) show prominent recent CL and several secondary follicles. (C) Most recent CL at the proestrus stage (upper right), a preovulatory follicle (left), and many recent CL. In the same rat as (C), the uterus was dilated (D), and mucification was observed in the vagina (D, insert), indicating synchronized histology at the proestrus stage in the implanted ovary, uterus, and vagina. (E) Cystic atretic follicles without CL. (F) Histology of implanted ovary in the OP-PND15 group was similar to that of ovaries in the OP-PND15 group rats without surgical operation (E). H-E staining. Bars in A, B, C, E and F are 50 micro-meter. Bar in D is 100 micro-meter. Bar in insert of D is 10 micro-meter.

In the transplanted ovaries in all groups, primary follicles were detected.

As for common histology of implanted ovaries, dilatation of the oviducts and inflammatory cell infiltration into ovaries and surrounding fibrosis were observed. There were no treatment- or surgery-related effects on other organs/tissues, including the brain, the pituitary, or the adrenal on morphological examination.

3.4. *Effect on ovulation and reproductive ability*

On the morning of estrus, the number of oocytes in the oviduct was counted (Table 3). The number in rats with normal cycling in the OP-PND5 group was comparable to that in the control group. No oocytes could be found in the oviduct of rats with abnormal cycling, including PE, in the OP-PND5 and OP-PND15 groups.

3.5. *Effect on reproductive ability*

Number of pups per litter, CL and implantation, ratios of the number of implantation sites per CL and pups per CL, body weights of pups, and relative ovarian weights in dams are shown in Fig. 4. All indicators of effects on reproduction and offspring were comparable between the control and OP-PND5 groups. Macroscopically, no abnormalities were detected in pups at termination.

4. Discussion

Transplantation of ovaries from donors to recipient ovariectomized rodents has been accepted as an effective method to clarify of which the hypothalamic–pituitary axis or the ovary is predominant in endocrinology field since 1960s [33]. Transplantation study of aged female rat ovaries to young ovariectomized rats showed folliculogenesis and ovulation indicating that old donor ovaries could begin to function in the young hosts.

The present study was conducted to determine whether it is the hypothalamic–pituitary axis or the ovary that is the primary mediator of induction of abnormal estrous cycling, both in the delayed effect and in defeminization, using ovarian exchange in rats postnatally exposed to OP, an estrogenic compound. The results indicate that estrous cycling is mainly controlled by recipient rats, i.e., normal cycling in control rats receiving control or OP-PND5 ovaries, gradually increased PE in OP-PND5 rats receiving control or OP-PND5 ovaries, and full-blown PE in OP-PND15 rats receiving control or OP-PND15 ovaries. The changes and timing of these events were similar to those in rats without ovary exchange in the control and OP-PND15 groups in the present study and in our previous study, where the same treatments were applied [13]. The results demonstrate that the hypothalamic–pituitary axis plays the predominant role in mediating the induction of abnormal estrous cyclicity for

Table 3
Number of oocytes at ovulation and ovary weights in Exp. 2.

Group	Estrous cycle	No. of oocytes	Body weight (g)	Ovary weight (mg)
Control	Normal (8)	12.3 ± 3.1	317.8 ± 18.2	120 ± 22
OP-PND5	Normal (7[a])	11.0 ± 2.1	301.6 ± 20.5	110 ± 2
	PE (7)	0	319.1 ± 10.2	75 ± 18*
OP-PND15	PE (8)	0	315.5 ± 13.1	64 ± 12*

PE, persistent estrus.
Numbers in parentheses indicate the number of rats examined.
[a] Oocytes could not be counted due to loss of oviduct in processing in one female.
*Significantly different value from the control group ($p < 0.01$).

both the delayed adverse effect and defeminization in rats postnatally exposed to OP.

Taking a few weeks to show normal cycling after ovarian exchange in the control and OP-PND5 groups indicates that transplanted ovaries in both the control and OP-PND 5 groups require a few weeks in order to work normally in subcutaneous tissue after exchange. The maintenance of normal function in the implanted ovaries for several months after the exchange was indicated by the morphologies of the transplanted ovaries. Histologically, the presence of most recent CL or preovulatory follicles indicates current ovulation in the most recent cycle and preparation for the next ovulation, suggesting normal cycling. Abundant recent CL indicate the occurrence of ovulation within recent estrous cycles. The synchronized histology of the implanted ovary, the uterus, and the vagina showing the same estrous cycle stage also supports the conclusion that the transplanted ovary was functional. On the contrary, the lack of any type of CL in ovaries transplanted from the control group to the OP-PND15 rats indicated that ovaries possessing normal functional potential were controlled by the recipient hypothalamus, resulting in the anovulatory status of the implanted ovaries in OP-PND15 rats. These results indicate that morphological changes in the transplanted ovaries are reflected by the endocrine environments of the recipients.

The similarity in the magnitudes of estrous cycling in the control and OP-PND15 rats receiving ovaries from the same or different groups to the corresponding rats without surgery and in our previous study [13] during the experimental period are indications that the implanted ovaries are under the control of recipients.

Although the recipient hypothalamic–pituitary axis is predominant over the implanted ovaries, the incomplete estrous cycling after transplantation and the increased numbers of abnormal cycling in control rats receiving OP-PND15 ovaries throughout the experiment period suggests that effects on the ovary by the postnatal exposure could not be excluded. Recently, increases in LHαgene expression were found in rat ovaries exposed to EE neonatally at the defeminization- and the delayed adverse effect-inducible doses [18]. These results suggest a possibility of weak but direct effect of the neonatal treatment on the ovary. Further investigation should be performed to identify any direct effects of postnatal exposure to estrogens on ovaries.

In the present study, we also investigated whether OP-PND5 treatment affected ovulation and reproductive abilities in young adult rats with normal cyclicity. No effects on ovulation or reproductive abilities were found in the present study, indicating the possibility that the dose inducing the delayed adverse effect does not affect either ovulation or reproductive ability. These results suggest that HPG axis control related to reproductive and/or ovulation ability might be normal, while normal estrous cyclicity is maintained in rats postnatally exposed to estrogens.

The precise target for the delayed adverse effects has not been fully determined yet; however, dysfunction of the LH surge center in the hypothalamus is presumed to be a powerful target for early onset of age-matched abnormal cycle, the most sensitive endpoint of the delayed adverse effect [20]. Kisspeptin, which is expressed in specific neurons in the anteroventral periventricular (AVPV) nucleus, is widely recognized as playing a crucial role in

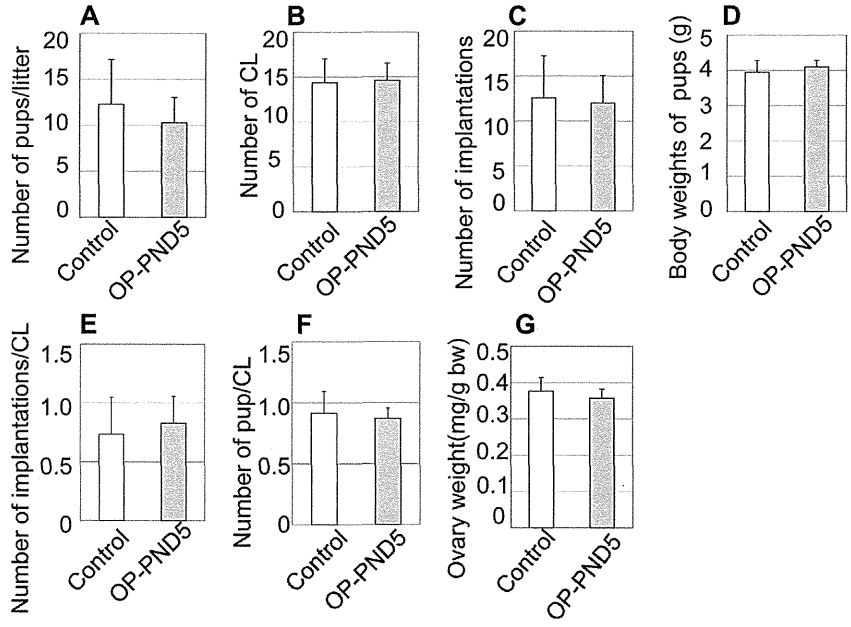

Fig. 4. Reproductive ability. Column and bar show mean and SD, respectively. (A–C) Numbers of pups, CL, and implantations per litter, respectively. (D) Body weights of pups. (E) and (F) Number of implantations per CL and pups per CL, respectively. (G) Relative ovarian weights in the dams.

ovulation and estrous cyclicity [34,35]. Kiss1 neurons in the AVPV express estrogen receptor α [36] and are considered to be a key to the LH surge. A number of studies of the effects of neonatal exposure to estrogens or estrogenic compounds on Kiss1 neurons in the hypothalamus have been reported using rodents [21]. We are also now investigating involvement of Kiss1 neurons in the AVPV in delayed adverse effects. OP-PND15 ovaries are impaired relative to control or OP-PND5 ovaries, indicating direct effects of OP on the ovary in rats. Follow-up work is needed to evaluate this phenomenon further and to determine the dose- and time-exposure response.

5. Conclusion

This ovarian exchange study indicates that the hypothalamic–pituitary axis, and not the ovary, might play the predominant role in mediating induction of abnormal estrous cycling in rats postnatally treated with OP to induce defeminization and the delayed adverse effect. During maintaining normal cycling, no effects on ovulation or reproduction ability were detected in rats postnatally exposed to OP.

Conflict of interest

The authors declare that there are no conflicts of interest. This study was partly supported by Health and Labor Sciences Research Grants, Research on Risk of Chemical Substances, Ministry of Health, Labor and Welfare, Japan (H25-Toxicol-003).

Transparency document

The Transparency document associated with this article can be found in the online version.

Acknowledgements

We thank Mss Ayako Saikawa and Yoshimi Komatsu for technical assistance in histopathological examination.

References

[1] Herbst AL. Stilbestrol and vaginal cancer in young women. CA Cancer J Clin 1972;22:292–5.
[2] Newbold RR, McLachlan JA. Vaginal adenosis and adenocarcinoma in mice exposed prenatally or neonatally to diethylstilbestrol. Cancer Res 1982;42:2003–11.
[3] Takasugi N, Tomooka Y. Alteration of the critical period for induction of persistent oestrus by early postnatal treatment with gonadal steroids in neonatally cortisone-primed mice. J Endocrinol 1976;69:293–4.
[4] Cheng HC, Johnson DC. Serum estrogens and gonadotropins in developing androgenized and normal female rats. Neuroendocrinology 1974;13:357–65.
[5] Dussault JH, Walker P, Dubois JD, Labrie F. The development of the hypothalamo–pituitary axis in the neonatal rat: sexual maturation in male and female rats as assessed by hypothalamic LHRH and pituitary and serum LH and FSH concentrations. Can J Physiol Pharmacol 1977;55:1091–7.
[6] Katsuda S, Yoshida M, Watanabe G, Taya K, Maekawa A. Irreversible effects of neonatal exposure to p-tert-octylphenol on the reproductive tract in female rats. Toxicol Appl Pharmacol 2000;165:217–26.
[7] Branham WS, Sheehan DM, Zehr DR, Medlock KL, Nelson CJ, Ridlon E. Inhibition of rat uterine gland genesis by tamoxifen. Endocrinology 1985;117:2238–48.
[8] Branham WS, Sheehan DM, Zehr DR, Ridlon E, Nelson CJ. The postnatal ontogeny of rat uterine glands and age-related effects of 17 beta-estradiol. Endocrinology 1985;117:2229–37.
[9] Yoshida A, Newbold RR, Dixon D. Abnormal cell differentiation and p21 expression of endometrial epithelial cells following developmental exposure to diethylstilbestrol (DES). Toxicol Pathol 2000;28:237–45.
[10] Yoshida M, Takenaka A, Katsuda S, Kurokawa Y, Maekawa A. Neonatal exposure to p-tert-octylphenol causes abnormal expression of estrogen receptor alpha and subsequent alteration of cell proliferating activity in the developing Donryu rat uterus. Toxicol Pathol 2002;30:357–64.
[11] Newbold RR, Bullock BC, McLachlan JA. Uterine adenocarcinoma in mice following developmental treatment with estrogens: a model for hormonal carcinogenesis. Cancer Res 1990;50:7677–81.
[12] Newbold RR, Jefferson WN, Padilla-Burgos E, Bullock BC. Uterine carcinoma in mice treated neonatally with tamoxifen. Carcinogenesis 1997;18:2293–8.
[13] Yoshida M, Katsuda SI, Tanimoto T, Asai S, Nakae D, Kurokawa Y, et al. Induction of different types of uterine adenocarcinomas in Donryu rats due to neonatal exposure to high-dose p-t-octylphenol for different period. Carcinogenesis 2002;23:1745–50.
[14] MacLusky NJ, Naftolin F. Sexual differentiation of the central nervous system. Science 1981;211:1294–302 [review].
[15] Mossbs CV, Kannergieter LS, Finch CE. Delayed anovulatory syndrome induced by estradiol in female C57BL/6J mice: age-like neuroendocrine, but not ovarian impairments. Biol Reprod 1985;32:1010–7.
[16] Zoeller RT, Brown TR, Doan LL, Gore AC, Skakkebaek NE, Soto AM, et al. Endocrine-disrupting chemicals and public health protection: a statement of principles from The Endocrine Society. Endocrinology 2012;153:4097–110.
[17] Gore AC, Walker DM, Zama AM, Armenti AE, Uzumcu M. Early life exposure to endocrine-disrupting chemicals causes lifelong molecular programming of the hypothalamus and premature reproductive aging. Mol Endocrinol 2011;25:2157–68.
[18] Nozawa K, Nagaoka K, Zhang H, Usuda K, Okazaki S, Taya K, et al. Neonatal exposure to 17α-ethynyl estradiol affects ovarian gene expression and disrupts reproductive cycles in female rats. Reprod Toxicol 2014;46:77–84.
[19] Shirota M, Kawashima J, Nakamura T, Ogawa Y, Kamiie J, Yasuno K, et al. Delayed effects of single neonatal subcutaneous exposure of low-dose 17α-ethynylestradiol on reproductive function in female rats. J Toxicol Sci 2012;37:681–90.
[20] Takahashi M, Inoue K, Morikawa T, Matsuo S, Hayashi S, Tamura K, et al. Delayed effects of neonatal exposure to 17 alpha-ethynylestradiol on the estrous cycle and uterine carcinogenesis in Wistar Hannover GALAS rats. Reprod Toxicol 2013;40:16–23.
[21] Usuda K, Nagaoka K, Nozawa K, Zhang H, Taya K, Yoshida M, et al. Neonatal exposure to 17α-ethinyl estradiol affects kisspeptin expression and LH-surge level in female rats. J Vet Med Sci 2014;76:1105–10.
[22] Yoshida M, Takahashi M, Inoue K, Hayashi S, Maekawa A, Nishikawa A. Delayed adverse effects of neonatal exposure to diethylstilbestrol and their dose dependency in female rats. Toxicol Pathol 2011;39:823–34.
[23] Ninomiya K, Kawaguchi H, Souda M, Taguchi S, Funato M, Umekita Y, et al. Effects of neonatally administered diethylstilbestrol on induction of mammary carcinomas induced by 7,12-dimethylbenz[A]anthracene in female rats. Toxicol Pathol 2007;35:813–8.
[24] Robinson J. Prenatal programming of the female reproductive neuroendocrine system by androgens. Reproduction 2006;132:539–47.
[25] Neal-Perry G, Santoro N. Chapter 50 Aging in the hypothalamic–pituitary–ovarian axis. In: Neill JD, editor. Knobil and Neill's physiology of reproduction, vol. 2. Amsterdam: Academic Press; 2006. p. 2729–55.
[26] Santoro N, Isaac B, Neal-Perry G, Adel T, Weingart L, Nussebaum A, et al. Impaired folliculogenesis and ovulation in older reproduction aged women. J Clin Endocrinol Metab 2003;88:5502–9.
[27] Burger HG, Hale GE, Dennerstein L, Robertson DM. Cycle and hormone changes during perimenopause: the key role of ovarian function. Menopause 2008;15:603–12.
[28] Hall JE. Neuroendocrine changes with reproductive aging in women. Semin Reprod Med 2007;25:344–51.
[29] Blake CA, Ashiru OA. Disruption of rat estrous cyclicity by the environmental estrogen 4-tert-octylphenol. Proc Soc Exp Biol Med 1997;216:446–51.
[30] Katsuda S-I, Yoshida M, Isagawa S, Asagawa Y, Kuroda H, Watanabe T, et al. Dose- and treatment duration-related effects of p-tert-octylphenol on female rats. Reprod Toxicol 2000;14:119–26.
[31] White R, Jobling S, Horare A, Sumpter JP, Parker MG. Environmental persistent alkylphenolic compounds are estrogenic. Endocrinology 1994;135:175–82.
[32] Yoshida M, Katsuda S, Ando J, Kuroda H, Takahashi M, Maekawa A. Subcutaneous treatment of p-tert-octylphenol exerts estrogenic activity on the female reproductive tract in normal cycling rats of two different strains. Toxicol Lett 2000;116:89–101.
[33] Gore AC. Aging and reproduction. In: Plant TM, Beleznik AJ, editors. Knobil and Neill's physiology of reproduction, 2, 4th ed. London: Academic Press; 2015. p. 1661–993.
[34] UenoyamaT. Tsukamura H, Maeda KI. Kisspeptin/metastin: a key molecule controlling two modes of ganadotropin-releasing hormone/luteinizing hormone release in female rats. J Neuroendocrinol 2009;21:299–304.
[35] Roa J, Navarro VM, Tena-Serpere M. Kisspeptins in reproductive biology: consensus knowledge and recent development. Biol Reprod 2011;85:650–60.
[36] Smith JT, Popa SM, Clifton DK, Hoffman GE, Steiner RA. Kiss1 neurons in the forebrain as central processors for generating the preovulatory luteinizing hormone surge. J Neurosci 2006;26:6687–94.

The Journal of Toxicological Sciences (J. Toxicol. Sci.)
Vol.40, No.6, 727-738, 2015

Original Article

Dose-dependent acceleration in the delayed effects of neonatal oral exposure to low-dose 17α-ethynylestradiol on reproductive functions in female Sprague-Dawley rats

Mariko Shirota[1], Jun Kawashima[1], Tomohiro Nakamura[1], Junichi Kamiie[2], Kinji Shirota[2,3] and Midori Yoshida[4]

[1]Laboratory of Comparative Toxicology, School of Veterinary Medicine, 1-17-71 Fuchinobe, Chuo-ku, Sagamihara, Kanagawa 252-5201, Japan
[2]Laboratory of Veterinary Pathology, Azabu University, 1-17-71 Fuchinobe, Chuo-ku, Sagamihara, Kanagawa 252-5201, Japan
[3]Research Institute of Biosciences, Azabu University, 1-17-71 Fuchinobe, Chuo-ku, Sagamihara, Kanagawa 252-5201, Japan
[4]Division of Pathology, National Institute of Health Sciences, 1-18-1 Kamiyoga, Setagaya-ku, Tokyo 158-8501, Japan

(Received June 25, 2015; Accepted August 28, 2015)

ABSTRACT — Xenoestrogen exposure during the critical period of sexual differentiation of the brain causes delayed effects on female reproduction. We investigated the internal dose of orally administered ethynylestradiol (EE) during the critical period and its delayed effects by administering 0 (vehicle control), 0.4, or 2 μg/kg EE to female Sprague-Dawley rats for 5 days from postnatal day (PND) 1. Determination of serum EE level 24 hr after the initial dosing and 6 and 24 hr after the final dosing of 2 μg/kg indicated that the administered EE entered the circulation and cleared after every administration. Although the treatment did not affect physical development, including growth, eyelid opening, and vaginal opening, the estrous cycle was arrested from postnatal week (PNW) 12 even with 0.4 μg/kg EE, with an inverse correlation between doses and arresting ages. Although ovarian morphology at PNW 22-23 indicated that the treatment caused long-term anovulation and cystic follicle formation, the number of primordial follicles at PNW 22-23 was similar among the groups. Because this number was lower than that at PND 10 in all groups, primordial follicles may have been consumed under long-term anovulation. The treatment also caused other abnormalities, including mammary gland hyperplasia, increase in pituitary and liver weights, and decrease in the uterine weight. Because the highest circulating EE level in the 2 μg/kg-treated neonates is considered to be comparable to the physiological range of estradiol-17β, we concluded that a slight increase in the circulating estrogens during the neonatal period exerts irreversible delayed effects.

Key words: 17α-ethynylestradiol, Internal dose level, Critical period, Sexual differentiation, Estrous cycle

INTRODUCTION

Critical periods for morphogenesis or functional differentiation in humans and animals are highly sensitive not only to their endogenous key molecules but also to exogenous analogues for such key molecules (McLachlan *et al.*, 2012). Among these key molecules, sex steroids are determinants of sexual phenotypes after organogenesis in vertebrates (Gore *et al.*, 2014; Chung and Anthony, 2013), and it has been well established that exposure to xenoestrogens, such as alkylphenols, synthetic estrogens, and phytoestrogens (Jefferson *et al.*, 2012) affects female reproductive function in rodents during the critical period of sexual differentiation (Frye *et al.*, 2012). In a previous study, we have found that a single s.c. injection of 17α-ethynylestradiol (EE) at a dose level up to 2 μg/kg on postnatal day (PND) 1 arrests the estrous cycle at younger ages and that treatment with a lower dose of EE lasts for a longer period until the arrest of estrous cycle (Shirota *et al.*, 2012). In that study, 0.08 μg/kg of EE at PND 1

Correspondence: Mariko Shirota (E-mail: m-shirota@azabu-u.ac.jp)

arrested the estrous cycle in some animals at 32 weeks of age, slightly younger than vehicle-treated animals. These findings suggest that the delayed effects of weak estrogens could be escaped from toxicological studies conducted under various safety test guidelines because the guidelines do not require monitoring the estrous cycle of the treated animals until middle age. The National Institute of Environment in Japan has confirmed estrogenic activity for more than 80 compounds among 273 candidate compounds. While the estrogenic activity of these compounds, except for synthetic estrogens, is generally weak, most of these compounds are orally exposed to humans and animals through food, as food contaminants, or as food ingredients, or medicine (Safe, 2000). However, only limited studies have been conducted on the effects of oral exposure (Ohta *et al.*, 2012; Cimafranca *et al.*, 2010; Prins *et al.*, 2011). Therefore, in the present study, we investigated the delayed effects of oral exposure to a low-dose estrogenic compound on reproductive functions in female Sprague-Dawley rats.

EE is a synthetic estradiol that is commonly used in formulating contraceptives. Since EE is able to exert estrogenic effects as endogenous estrogens do, it has been used as a positive control compound in evaluating the estrogenic activity of various xenobiotics. Compared with estradiol-17β, the binding affinity of EE with recombinant full-length human estrogen receptor (ER) α is estimated to be 56% (Freyberge *et al.*, 2010). Agonistic activity of EE mediated by human ER α was estimated to be approximately 35 times higher than that by human ER β by the assay using cell-lines co-expressing a reporter and either receptor (Barkhem *et al.*, 1998). The relative *in vitro* estrogenic activity of EE to estradiol-17β is varied among studies. While the reported lowest value was 50% (Nakamuro *et al.*, 2002), most of *in vitro* studies estimated the value ranged 90-250% (Soto *et al.*, 1995; Coldham *et al.*, 1997; Fang *et al.*, 2000; Nishihara *et al.*, 2000; Sanseverino *et al.*, 2009).

However, the binding affinity of EE with rat α-fetoprotein, a major transport protein found in the serum of fetal and neonatal rats (Gitlin and Boesman, 1967), is approximately 100 times lower than that with estradiol-17β (Hong *et al.*, 2012). Therefore, orally administered EE is expected to pass through the blood-brain barrier of neonates as xenoestrogens do if EE reaches the circulation. Therefore, in the present study, we determined the circulating level of EE after dosing to provide information on the relationship between the internal dose of EE and delayed effects for further evaluation of the delayed effects of xenoestrogens.

MATERIALS AND METHODS

Test compound

EE (CAS #57-53-6, Sigma-Aldrich Japan, Tokyo, Japan) was dissolved in ethanol (Wako Pure Chemical Industries, Osaka, Japan) at a concentration of 100 mg/mL, following which the solution was diluted with corn oil (Wako Pure Chemical Industries) to formulate EE at a constant volume of 10 mL/kg.

Doses of EE

Doses of EE in the present study were set at 0.4 and 2 μg/kg/day because we had already confirmed that s.c. injection of 0.4 and 2 μg/kg of EE significantly alters the estrous cycle. Therefore, we adopted identical dose levels to the previous study at a daily dose or an accumulated dose for 5 days.

Experimental design

Procedures for animal experiments described below have been approved by the Committee of Animal Experiments at Azabu University. Female neonates were obtained through spontaneous delivery from pregnant Sprague-Dawley rats [Crl:CD(SD)IGS], which were purchased from Charles River Japan (Kanagawa, Japan) or were obtained by mating with adult male Crl:CD(SD)IGS rats purchased from the same breeder. The animals were maintained under a lighting condition (lights on 08:00-20:00) in an animal husbandry facility, which was controlled for the standards of temperature and humidity at 21 ± 1°C and 50-60%, respectively. The animals were housed in a plastic cage with bedding materials (Sunflake; Oriental Kobo, Tokyo, Japan) with pellet chow (CE-2; Clea Japan, Tokyo, Japan) and tap water (Kanagawa Prefectural Government, Kanagawa, Japan) *ad libitum*. The pregnant animals were daily monitored for delivery from gestational day 20, and the day when neonates were confirmed by 16:00 was designated as PND 0. The neonates were collected and assigned to each treatment group at PND 1. This study consisted of main and satellite experiments. The main experiment was performed to examine delayed effects of orally administered EE from PND 1 to 5, the period of steroid sensitivity for female fertility (Barraclough, 1961; Gorski, 1968), using 45 female neonates from 7 dams. The satellite experiment was performed to determine the circulating EE levels after the initial and the final oral administration of EE to 32 female neonates from 7 dams. All groups of the neonates were identified by a tattoo, and those in the main study were placed under the same dams to equalize maternal effects on them. The litter size was adjusted to 8 female neonates